An integrated EEG-fNIRS-based Vector-Phase Analysis for early hemodynamic response: Applications to BCI

Author

ARSHIA ARIF

Regn Number

277309

Supervisor

DR. JAWAD KHAN

DEPARTMENT OF ROBOTICS AND ARTIFICIAL INTELLIGENCE

SCHOOL OF MECHANICAL & MANUFACTURING ENGINEERING

NATIONAL UNIVERSITY OF SCIENCES AND TECHNOLOGY

ISLAMABAD

NOVEMBER,2020

An integrated EEG-fNIRS based Vector Phase Analysis for hemodynamic response detection with applications to BCI

Author

ARSHIA ARIF

Regn Number

277309

A thesis submitted in partial fulfillment of the requirements for the degree of

MS Mechanical Engineering

Thesis Supervisor:

DR. M. JAWAD KHAN

Thesis Supervisor's Signature: _____

DEPARTMENT OF ROBOTICS AND ARTIFICIAL INTELLIGENCE

SCHOOL OF MECHANICAL & MANUFACTURING ENGINEERING

NATIONAL UNIVERSITY OF SCIENCES AND TECHNOLOGY

ISLAMABAD

NOVEMBER,2020

Declaration

I certify that this research work titled "*An integrated EEG-fNIRS based Vector Phase Analysis for hemodynamic response detection: Applications to BCI"* is my own work. The work has not been presented elsewhere for assessment. The material that has been used from other sources it has been properly acknowledged / referred.

Signature of Student

ARSHIA ARIF

00000277309

Plagiarism Certificate (Turnitin Report)

This thesis has been checked for Plagiarism. Turnitin report endorsed by Supervisor is attached.

Signature of Student

ARSHIA ARIF

Registration Number 277309

Signature of Supervisor

Copyright Statement

- Copyright in text of this thesis rests with the student author. Copies (by any process) either in full, or of extracts, may be made only in accordance with instructions given by the author and lodged in the Library of NUST School of Mechanical & Manufacturing Engineering (SMME). Details may be obtained by the Librarian. This page must form part of any such copies made. Further copies (by any process) may not be made without the permission (in writing) of the author.
- The ownership of any intellectual property rights which may be described in this thesis is vested in NUST School of Mechanical & Manufacturing Engineering, subject to any prior agreement to the contrary, and may not be made available for use by third parties without the written permission of the SMME, which will prescribe the terms and conditions of any such agreement.
- Further information on the conditions under which disclosures and exploitation may take place is available from the Library of NUST School of Mechanical & Manufacturing Engineering, Islamabad.

Acknowledgements

I am thankful to my Creator Allah Subhana-Watala to have guided me throughout this work at every step and for every new thought which You setup in my mind to improve it. Indeed I could have done nothing without Your priceless help and guidance. Whosoever helped me throughout the course of my thesis, whether my parents or any other individual was Your will, so indeed none be worthy of praise but You.

I am profusely thankful to my beloved parents who raised me when I was not capable of walking and continued to support me throughout in every department of my life.

I would also like to express special thanks to my supervisor Dr. Jawad Khan for his help throughout my thesis and also for Rehabilitation and Assistive Robotics and Computer Vision courses which he has taught me. I can safely say that I haven't learned any other engineering subject in such depth than the ones which he has taught. Each time I got stuck in something, he came up with the solution. Without his help I wouldn’t have been able to complete my thesis. I appreciate his patience and guidance throughout the whole thesis.

I would also like to thank my GEC members Dr. Hasan Sajid, Dr. Karamdad and Dr. Noman Naseer for being on my thesis guidance and evaluation committee and express my special thanks to Dr. Noman Naseer for his help.

Finally, I would like to express my gratitude to all the individuals who have rendered valuable assistance to my study.

Dedicated to my exceptional parents and adored siblings whose tremendous support and cooperation led me to this wonderful accomplishment.

Abstract

Objective. In this thesis, a novel methodology for better hemodynamic response detection, has been developed using multimodal brain-computer interface (BCI). *Methodology Used*. A novel classifier has been developed for achieving better classification accuracy using two modalities. An integrated EEG-fNIRS based Vector phase analysis (VPA) has been conducted. An online available dataset assembled at the Technische Universität Berlin; comprising of simultaneous fNIRS and EEG signals of 26 physically and mentally fit persons during n-back tasks has been used for this research. Instrumental and physiological noise removal has been done using preprocessing techniques followed by detection of activity in both modalities individually. VPA, with resting state threshold circle, is used for detection of hemodynamic response in functional near-infrared spectroscopy (fNIRS) data whereas phase plots for electroencephalography (EEG) signals have been constructed using Hilbert Transform to detect the activity in each trial. Multiple threshold circles are drawn in the vector plane, where each circle is drawn after task completion in each trial of EEG signal. Finally, both processes are integrated in one vector phase plot to get combined detection of hemodynamic response for activity. *Main Results.* Results of this study illustrates that the combined EEG-fNIRS VPA yields considerably higher average classification accuracy, that is 91.35%, as compared to other techniques that are Convolutional neural network (CNN), Support vector machine(SVM) and VPA (with dual threshold circles) with classification accuracies 89%, 82% and 86% respectively. *Significance.* Outcomes of this research demonstrate that improved classification performance can be feasibly achieved using multimodal VPA for EEG-fNIRS hybrid data.

Key Words: *EEG-fNIRS Hybrid BCI, Vector Phase Analysis, Hemodynamic response detection*

Table of Contents

List of Figures

List of Tables

CHAPTER 1: INTRODUCTION

The research work presented in this dissertation is based on hybrid brain computer interface (BCI) systems. Classification accuracy of the system has been improved by designing a novel classifier based on vector phase analysis (VPA). EEG and fNIRS signals have been used for this purpose. Activity detection has been done using EEG signals individually at first. Then an integrated EEG-fNIRS-based VPA is designed to improve the accuracy of hemodynamic response detection.

1.1 Brain computer interface:

Brain–Computer Interface (BCI) is a pathway between computer and brain that permits the control of a computer application by brain activity. (Vidaurre, C., & Blankertz, B., 2010). The main purpose of BCI is to equip the physically impaired people, especially with motor disabilities, with the facility to communicate with the help of their brain signals. (Nicolas-Alonso, L. F. and Gomez-Gil, J., 2012). BCI helps the user to develop an interface between their brain and peripheral devices without any kind of physical movement (Allison, B. et al.,2010). Various assistive rehabilitative devices have been controlled using different types of BCI systems, for instance electroencephalography (EEG) (AL-Quraishi et al. 2018, Beyrouthy, T., 2016), electromyography (EMG) (Naseer. N. et al., 2018, D. Farina et al.,2014), electrocorticography (ECoG) (Yanagisawa et al., 2012) and functional near-infrared spectroscopy (fNIRS) (Khan, R.A., Naseer, N., Qureshi, N.K. et al. 2018) etc. There are two main categories of BCI systems depending upon the part of body from where the signal is being recorded. First is direct BCI, in case the signal is recoded directly from the brain, and the second is indirect BCI, in case the signal is collected from the nervous system or the peripheral muscles. Further categories of BCI system used to assess the brain signal, are invasive, semi-invasive and non-invasive. Invasive BCIs e.g. targeted muscle reinnervation and implanted microelectrode array give better signal strength but the disadvantages of these BCI systems are in monitoring of localized brain activity, surgical process involvement, and build-up of scar tissue. In semi-invasive BCI system, ECog is employed to acquire brain signals after electrodes are implanted beneath the skull. Whereas, in non-invasive BCIs such as EEG, functional magnetic resonance imaging (fMRI) and fNIRS, data is acquired without any surgery or implantation using wearable

devices. Due to the advantages of non-invasive BCIs that they are portable and no implantation is required, they preferred over the other types of BCI systems, despite the fact that signal recorded using non-invasive BCIs are of low strength in comparison to semi-invasive and invasive BCIs. (Nazeer et al., 2020)

A BCI system consists of five phases: i) acquisition of brain signals, ii) preprocessing, iii) feature extraction, iv) classification, and v) application interface (Naseer and Hong, 2015). In the first step signals from brain are acquired by using suitable modality for brain imaging. Secondly using preprocessing, instrumental and physiological noises are removed by filtering and de-trending. Various methods can be applied for extraction of features in third step. Keeping in mind the number of channels, data size and quantity of trials, appropriate type of features can be selected. By the usage of appropriate classification algorithm, signals are predominantly decoded in fourth step. To control external devices, the signals after classification are sent to the controlling entity, for generating controlling commands in the final step. (Nazeer et al., 2020)

1.1.1 Hybrid BCI:

In this research, we intend to use hybrid BCI. A hybrid BCI system is usually comprised of two BCIs. It can also be composed of at least one BCI and another system. It can also have one brain signal and a non-brain signal as its input. A hybrid system can operate sequentially or simultaneously. In case of parallel functioning the inputs are processed at the same time whereas in sequential operation first input serves as a “Brain switch”. A hybrid BCI is expected to achieve better performance and classification accuracy than other conventional systems. (Pfurtscheller,G. et al., 2010)

EEG and fNIRS are two of the major non-invasive BCIs. EEG is a signal formed by the field potential generated as a result of collective and synchronous action of neurons. As a non-invasive BCI, voltage fluctuations can be recorded using electrodes placed along the scalp. (Blinowska, K. and Durka, P. 2006).

fNIRS is one of the emerging BCIs which records the brain activity as blood oxygen level changes. Near-infrared-range light with wavelength 650~1000 nm is used to estimate the deoxygenated hemoglobin (HbR) and oxygenated hemoglobin (HbO) concentration changes (Villringer, A. et al., 1993)

Both have their own strengths and draw backs. For example, EEG possesses good temporal resolution (~0.05s) whereas fNIRS's temporal resolution (~1s) is just moderate. Furthermore, EEG provides poor spatial resolution (~10mm) while fNIRS offers good spatial resolution (~5mm). (Nicolas-Alonso and Gomez-Gil, 2012)

1.2 Previous Work:

Vector phase analysis (VPA) displays the trajectory formed as a result of deoxy-hemoglobin (ΔHbR) and oxy-hemoglobin (ΔHbO) changes(Zafar, A. & Hong, K. S., 2018).Magnitude and angle are calculated using ΔHbO and ΔHbR, which are used to construct a two-dimensional vector plane(Nazeer et al., 2020). This plane is split up into 8 phases for the classification of hemodynamic response (Kato, T., 2019). A threshold circle is plotted on the vector plane to detect the brain activity (Hong, K.S. & Naseer, N., 2016). This method has already been used for neuronal activation detection (Zafar, A. & Hong, K.S., 2018), initial dip detection in hemodynamic response (Zafar, A. & Hong, K. S., 2018, Zafar, A. & Hong, K. S., 2016, Yoshino & Kato, 2012, Hong, K.S. and Zafar, A., 2018), reduction of delay in initial dip detection (Hong, K. S., Naseer, N., 2016), oxygen level detection in prefrontal cortex (Sano, M. et al., 2013) and determining the brain region of interest for BCI (Hong, K. S., Khan, M. J. and Hong M. J., 2018). Table 1-1 shows the literature review and previous work done related to this research.

VPA, with dual threshold circles, has been used for the early hemodynamic response detection using EEG. The second threshold circle has been drawn using ΔHbO and ΔHbR magnitudes during the time span when a noticeable EEG activity has been sensed. During this time window highest EEG power has been used as a criterion to select the corresponding HbO and HbR magnitudes, which are then further used to determine the magnitude of second circle. The accuracy reported with this technique is 86% (Khan. M. J. et al., 2018). The average classification accuracies on multimodal (n-back test) dataset using SVM, and CNN are reported to be 82% and 87-89% respectively (Saadati et al., 2020, Asgher et al., 2020, Saadati et al., 2020). Average classification accuracy for event related potential (ERP) analysis has turned out to be 76.5±8% (Shin, J. et al., 2018).

Table 1.1: Literature Review

S No.	Title of Paper	Stimulation	Area	Detection Method
1	Feature Extraction and Classification methods for Hybrid fNIRS-EEG Brain-Computer Interfaces	Mental arithmetic and word formation tasks for LIS	Prefrontal cortex	Vector Phase Analysis. LDA for classification
2	Neuronal activation detection using vector phase analysis with Dual threshold circles: a functional near-infrared spectroscopy Study	Two finger tapping tasks (right-hand thumb and little finger)	Left Motor Cortex	Vector phase analysis with Dual threshold circles
3	Existence of Initial Dip for BCI: An Illusion or Reality (2018)	-	-	ISOI, FMRI, fNIRS (Vector based phase analysis)
4	Detection and classification of three-class initial dips from prefrontal cortex (2017)	Mental arithmetic, mental counting, puzzle solving, finger tapping, finger poking, and visual stimulus tasks	Prefrontal, motor, somatosensory, and visual cortex	Vector phase analysis with a threshold circle
5	Increased oxygen load in the prefrontal cortex from mouth breathing: a vector-based near-infrared spectroscopy study (2013)	Nasal and mouth breathing task	Prefrontal cortex	Vector based Phase Analysis
6	Vector-based phase classification of initial dips during word listening using near-infrared spectroscopy (2012)	Single word listening task	Auditory Cortex	Vector based Phase Analysis
7	Early Detection of Hemodynamic Responses Using EEG: A Hybrid EEG-fNIRS Study (2018)	Thumb tapping	Motor cortex	Vector based phase analysis with dual threshold circles & EEG power
8	Reduction of Delay in Detecting Initial Dips from Functional Near-Infrared Spectroscopy Signals Using Vector-Based Phase Analysis (2016)	Mental arithmetic and finger tapping tasks	Prefrontal and motor cortex	Vector phase analysis with a threshold circle

1.3 Problem Statement:

- For BCI systems, it is very important to have an accurate and less complex architecture to control a device with enhanced accuracy and real-time control.
- Integrating EEG with fNIRS resolves the accuracy problem, however, the time forcommand generation is significantly increased because of the inherent delay in fNIRS signal.
- There is a need for development of a hybrid EEG-fNIRS architecture that can enhance the accuracy along with minimal command generation time for better performance for control of devices.

1.4 Approach Used:

In this research, we propose a novel modified multimodal VPA methodology for the detection of activity in hemodynamic response. For the presented methodology, we have used hybrid BCI

(EEG-fNIRS) data for n-back test. Complete data has been preprocessed using conventional ways to make it noise free. Initially, both the modalities have been dealt with individually. Hilbert transform has been applied to EEG signals to get the required magnitude and phase values for the construction of polar plots for all the trials. Activity detection is made possible using these polar plots. Similarly, VPA has been applied to fNIRS signals for the construction of vector-based phase plot for hemodynamic response detection with resting state threshold circle as a detection criterion. Finally, an integrated multimodal VPA has been designed with multiple threshold circles, based on the activity completion of each EEG signal trial, to achieve better detection of hemodynamic response. Workflow for this research is shown in Figure 1.1

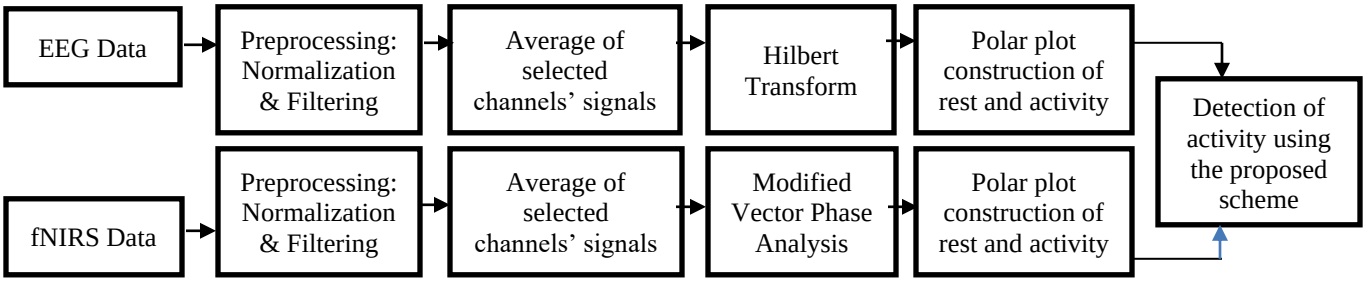

Figure 1.1: Workflow for this research

1.5 Objectives:

The objectives for this research are as under:

- Detection of activity in EEG signals using Hilbert Transform
- Detection of activity in hemodynamic response using EEG based circles on Vector phase plot made using fNIRS signals
- Calculation of combined accuracy using both modalities

1.6 Thesis Overview:

In this thesis, flow of work has been defined such as Chapter 2 contains the theory of all the methods used to design this classifier. It includes all the theoretical concepts for understanding the proposed scheme. Chapter 3 consists of the approach that has been used to achieve our objectives. It also includes the details of experimental paradigm and the algorithm developed to design the classifier. Chapter 4 contains the step wise results acquired for the complete

methodology Chapter 5 includes the discussion for this proposed scheme, Chapter 6 contains the conclusion of the thesis and Chapter 7 explains the future work briefly.

CHAPTER 2: THEORY

2.1 Hilbert Transform:

In this research, we have used Hilbert Transform (HT) for the calculation of the imaginary component of EEG signals along with their phases and magnitudes. Polar plot construction for each trial of each series of all EEG signals would then be achieved for the detection of activity.

For an EEG signal x(t), the imaginary component y(t) can be calculated using HT (Clercq, W. et al. 2003) as follows:

$$\boldsymbol{H[x(t)] = y(t) = \frac{1}{\pi}\int_{-\infty}^{\infty} \frac{x(\tau)}{t-\tau} d\tau} \quad (1)$$

Then the analytical signal corresponding to x(t), can be stated as:

$$\boldsymbol{z(t) = x(t) + iy(t) = a(t)e^{i\theta(t)}} \quad (2)$$

where y(t) and x(t) are complex conjugates of each other and the magnitude a(t) and phase θ(t) are defined as

$$\boldsymbol{a(t) = (x^2 + y^2)^{1/2}} \quad (3)$$

and

$$\boldsymbol{\theta(t) = tan^{-1}\frac{y(t)}{x(t)}} \quad (4)$$

Outcomes of HT are used to construct the polar plots of EEG signal trials for the indication of activity. We calculate the mean values, for both (x and y) coordinates using the complete trajectory in the phase plot, as $mean_x$ and $mean_y$ respectively. In this research we have set the criterion that if $mean_x$ is greater than 0 then it would be considered as the occurrence of activity (more explanation in the next section with results).

2.2 Vector-Phase Analysis:

Vector-phase analysis is a technique which can be used to detect the hemodynamic response by using just the two components, HbO and HbR, of fNIRS signals (Khan, M. J. et al., 2018). In this method there is a vector plane which is basically based on two orthogonal axes with HbO values at x-axis and HbR values at y-axis. This plane is split up into 8 phases (Yoshino & Kato, 2012; Sano et al., 2013; Yoshino et al., 2013; Oka et al., 2015) by getting two more axes in the plane. When the HbO and HbR plane is rotated counterclockwise by 45˚, the other two axes, i.e. COE

(cerebral oxygen exchange) and HBT (total hemoglobin), come into existence. ΔHBT and ΔCOE can be defined as:

$$\Delta \boldsymbol{HBT} = \frac{\Delta \boldsymbol{HbO} + \Delta \boldsymbol{HbR}}{\sqrt{\mathbf{2}}} \quad (5)$$

$$\Delta \boldsymbol{COE} = \frac{\Delta \boldsymbol{HbR} - \Delta \boldsymbol{HbO}}{\sqrt{\mathbf{2}}} \quad (6)$$

Phase and magnitude of a vector v = (ΔHbR, ΔHbO) expressed in this vector-plane are computed as follows:

$$|\boldsymbol{v}| = \sqrt{\Delta \boldsymbol{HbO}^{\mathbf{2}} + \Delta \boldsymbol{HbR}^{\mathbf{2}}} \quad (7)$$

$$\angle \boldsymbol{v} = \boldsymbol{tan}^{-\mathbf{1}}\left(\frac{\Delta \boldsymbol{HbR}}{\Delta \boldsymbol{HbO}}\right) = \boldsymbol{tan}^{-\mathbf{1}}\left(\frac{\Delta \boldsymbol{COE}}{\Delta \boldsymbol{HBT}}\right) + \mathbf{45°} \quad (8)$$

The eight phases of this vector plane are as shown in Figure 2.1

A threshold circle is drawn based on the maximum value of rest period in a signal. If the trajectory of ΔHbO and ΔHbR crosses this threshold circle, then this indicates the presence of activity. Magnitude values less than this threshold circle are counted as resting state (Hong and Naseer, 2016; Hong and Zafar, 2018; Kato, 2019). Initial dip and hemodynamic response can be detected in these eight phases. Phase (1-5) are there for initial dip detection whereas, phase(6-8) are there for the detection of hemodynamic signal(Hong and Zafar, 2018).

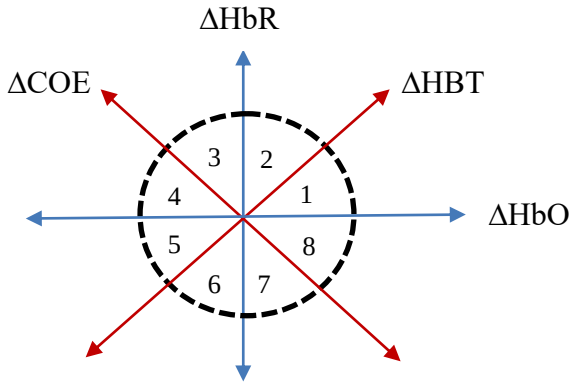

Figure 2.1: Vector phase plot configuration displaying 8 phases. Black dotted circle is the threshold circle for the detection of activity.

2.3 Ideal Hemodynamic Response Function (HRF):

For this novel technique we have used two gamma functions to construct the ideal trajectory of ΔHbO and ΔHbR (Khan, M. J. et al., 2018) as shown in Figure 2.2. Convolution of a canonical hemodynamic response function (cHRF) (i.e. *H(k))* with the stimulus *S(k)* is called designed hemodynamic response function (dHRF). The cHRF is constructed using the linear combination of two gamma variant functions as follows:

$$H(k) = \alpha_1 \left[\frac{{}^{k}/_{\tau_1}{}^{(\varphi_1 - 1)} e^{-({}^{k}/_{\tau_1})}}{\tau_1(\varphi_1 - 1)!} - \alpha_2 \frac{{}^{k}/_{\tau_2}{}^{(\varphi_2 - 1)} e^{-({}^{k}/_{\tau_2})}}{\tau_2(\varphi_2 - 1)!} \right] \tag{9}$$

where α_1 represents the amplitude, ϕ_i and τ_i (i = 1, 2) are for the tuning of scale and shape, respectively. α_2 represents the ratio of the response to undershoot.

The dHRF can be mathematically stated as follows:

$$dHRF(k) = \sum_{n=0}^{k-1} H(n)S(k-n) \tag{10}$$

Where *S(k)* is an impulse stimulus for each trial indicating rest and activity as

$$S(k) = \begin{cases} 1, \text{ if } k \in activity \\ 0, \text{ if } k \in rest \end{cases} \tag{11}$$

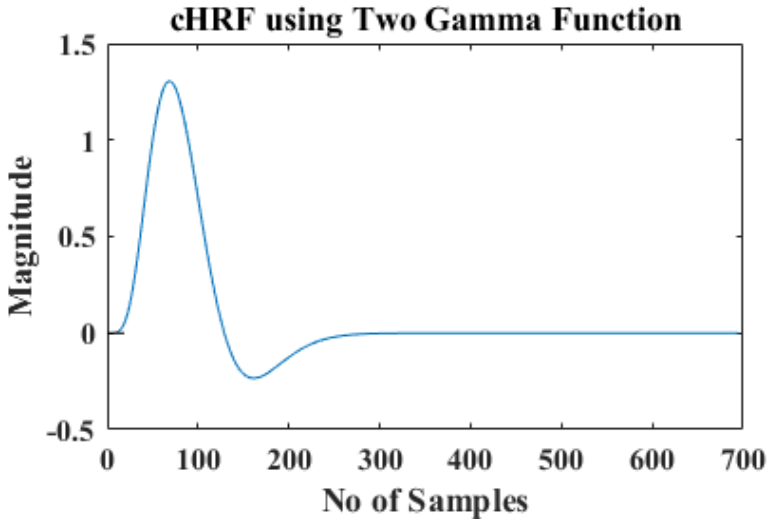

Figure 2.2: cHRF plotted using Two Gamma Function

CHAPTER 3: PROPOSED METHODOLOGY

3.1 Experimental Setup:

3.1.1 Subjects/Participants:

An open-source dataset has been used for this research. Data has been collected at Technische Universität Berlin. Twenty-six subjects, with average age of almost 26.1±3.5 years, who participated in this data collection, were healthy right-handed people. 9 of them were males and 17 were females. None of them possessed any mental, neuronal, or brain-related disorder. A written consent was given by all the participants after informing them about the complete experimental procedure. (Shin, J. et al., 2018).

3.1.2 Experimental paradigm:

Each participant was provided with an armchair to sit in front of a 24'' LCD display. Distance among the person's eyes and the display screen was 1.2m. The right armrest had numeric keypad buttons (number 7 and 8) attached with it. All persons were directed to see the display screen and try to abstain from moving their body. This experiment comprised of three types of tasks (n-back tasks, discrimination/selection response tasks and word generation tasks) with three sessions each. For this study we have used n-back task dataset (Shin, J. et al., 2018).

3.1.3 Dataset: n-back:

This dataset of n-back test was comprised of three sessions for every subject as shown in Figure 3.1, where every session had nine series of three types i.e. 0-,2- and 3-back tasks, in a counterbalanced order. Every series consisted of 2sec instruction time, displaying the kind of series (0-,2- and 3-back), followed by a 40sec time for task, 1s time for "STOP" word and a 20sec rest period. Hence, each series was composed of total 63sec.

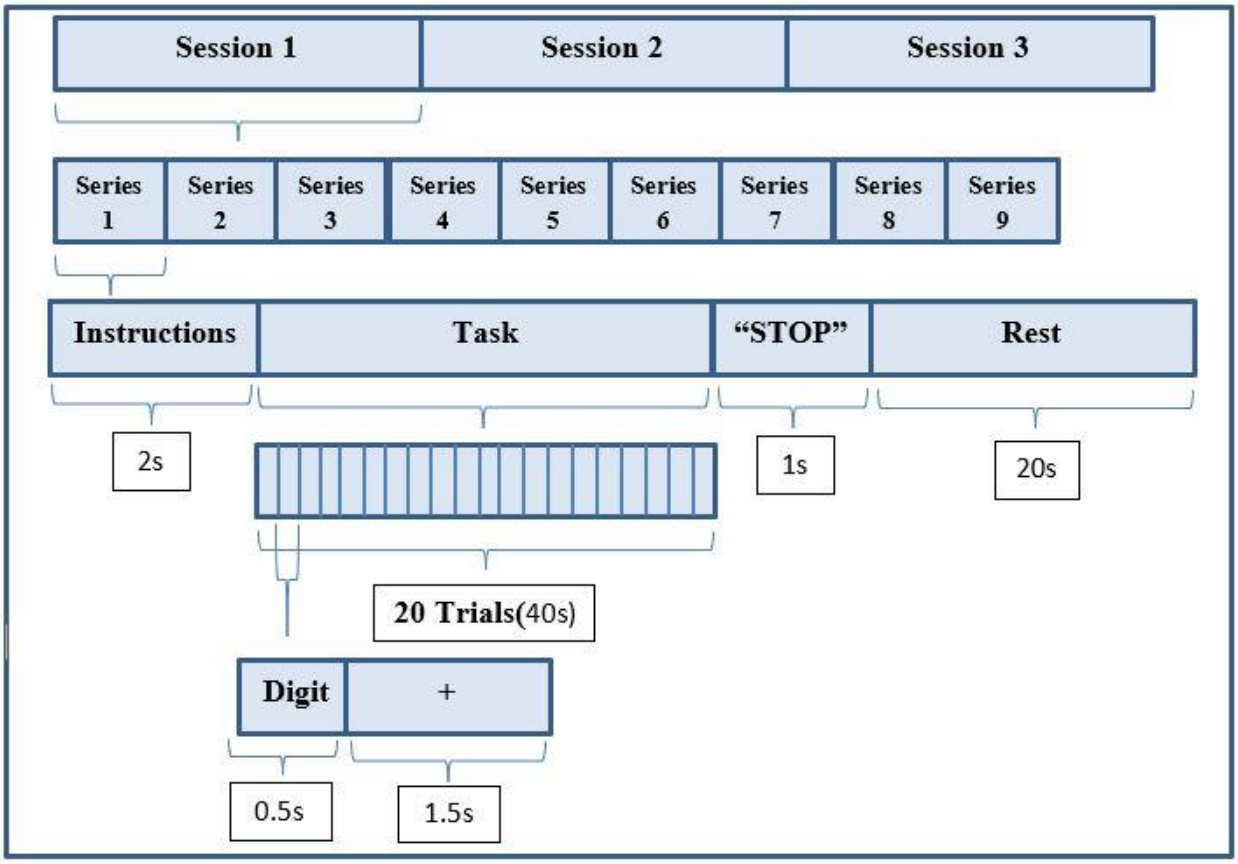

Figure 3.1: Experimental Paradigm for n-back task. Total 3 sessions were conducted with 9 series each and each series was comprised of initial 2s of instruction about the kind of task(0- ,2- and 3-back), 40s time for task, 1s of "STOP" word shown and 20s of rest. Task period had 20 trials in it and each trial of total 2s consisted of 0.5s of digit display and 1.5s of fixation

A short beep of 250ms was used to signify the person about the starting and end of every task duration. A cross was shown on the screen for the rest duration. Every task duration consisted of twenty trials, each of 2s. In every trial, a random digit was displayed on the screen for 0.5s and then a cross was displayed for 1.5s. For 0-back test, participants pressed either number 7 button for a 'target' digit or number 8 button for a 'non-target' digit. In case of 2- and 3- back tasks, participants were instructed to select the 'target' button, number 7, if presently shown digit was same as the 2 or 3 preceding digits respectively, otherwise the 'non-target' button, number 8. For each type of n-back task, total 180 trials were carried out (3 session X 3 series X 20 trials) (Shin, J. et al., 2018).

3.2 Acquisition and Processing of Data:

3.2.1 Data acquisition and channel configuration:

EEG and fNIRS signals were acquired in parallel. EEG data was acquired at the sampling frequency of 200Hz with the help of multichannel BrainAmp EEG amplifier (Brain Products GmbH, Gilching, Germany). According to international 10-5 system, thirty electrodes were attached to a flexible fabric cap (EASYCAP GmbH, Herrsching am Ammersee, Germany) as shown in Figure 2 (AFF5h, AFF6h, AFz, Fp1, Fp2, F1, F2, FC1, FC2, FC5, FC6, Cz, C3, C4, CP1, CP2, CP5, CP6, T7, T8, O1, O2, Pz, P3, P4, P7, P8, POz, TP9 (reference) & TP10 (ground)). Electrooculogram (EOG) was also measured using EEG amplifier. EOG was also acquired, at the same sampling frequency as EEG, with the help of 2 vertical and 2 horizontal electrodes. Out of all these channels seven frontal channels (Fp1, Fp2, F1, F2, AFF5h, AFF6h, AFz) were used for this study. We have chosen the frontal channels because n-back task is a cognitive task and its activity signals were expected to appear in the frontal cortex (Shin, J. et al., 2018).

fNIRS data was acquired at the sampling frequency of 10Hz with a NIRScout (NIRx Medizintechnik GmbH, Berlin, Germany). 16 sources and 16 detectors were attached at frontal (16 channels around AF3, AF4, AF7, AF8 and AFz), parietal (4 channels each around P3 and P4), motor (4 channels each around C3 and C4), and occipital (4 channels around POz) regions. An adjoining source-detector pair sets up an fNIRS channel. Configuration of a total of 36 channels was formed. The fNIRS channels were configured according to international 10-5 system around AF1, AF2, AF7, AF8, AF5h, AF6h, AFpz, AFp3, AFp4, AFp7, AFp8, AFFz, AFF3h, AFF4h, AFF5h, AFF6, C3h, C4h, C5h, C6h, CCP3, CCP4, CPP3, CPP4, FCC3, FCC4, PPOz, PPO3, PPO4, P3h, P4h, P5h, P6h, PO1, PO2, and POOz as shown in Figure 3.2. For this configuration, the distance among source and detector was set to 30mm for every channel. Figure 3.2 displays the channel configuration for EEG and fNIRS (Shin, J. et al., 2018).

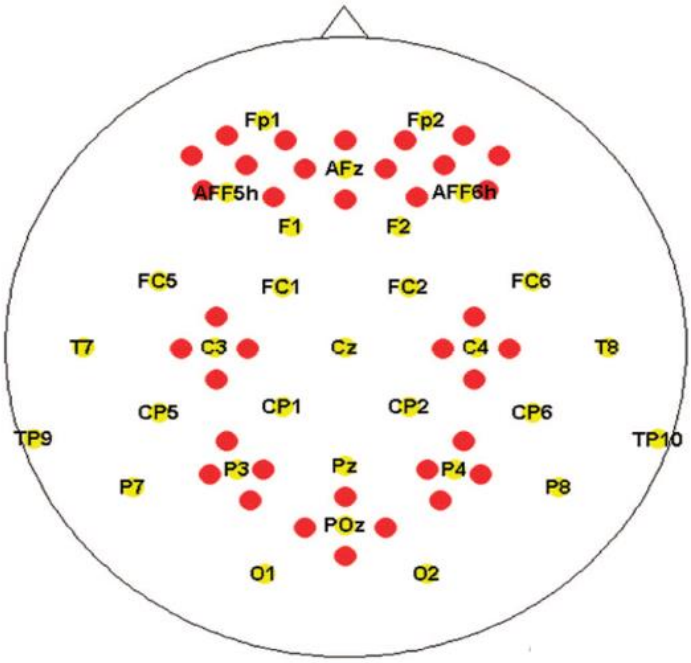

Figure 3.2: Channel configuration of EEG and fNIRS. Yellow circles denote the EEG channels whereas red circles denote the fNIRS channels (Shin, J. et al., 2018).

Twelve frontal channels (i.e.AF1, AF2, AFF5, AFF6, AFFz, AFpz, AFp3, AFp4, AF5h, AF6h, AFF3h, AFF4h) were used for this study based on the activity signal appearance in their hemodynamic response, as can be seen clearly from their VPA diagrams for all types of tasks(0-,2- and 3-back) in Figure 3.3.

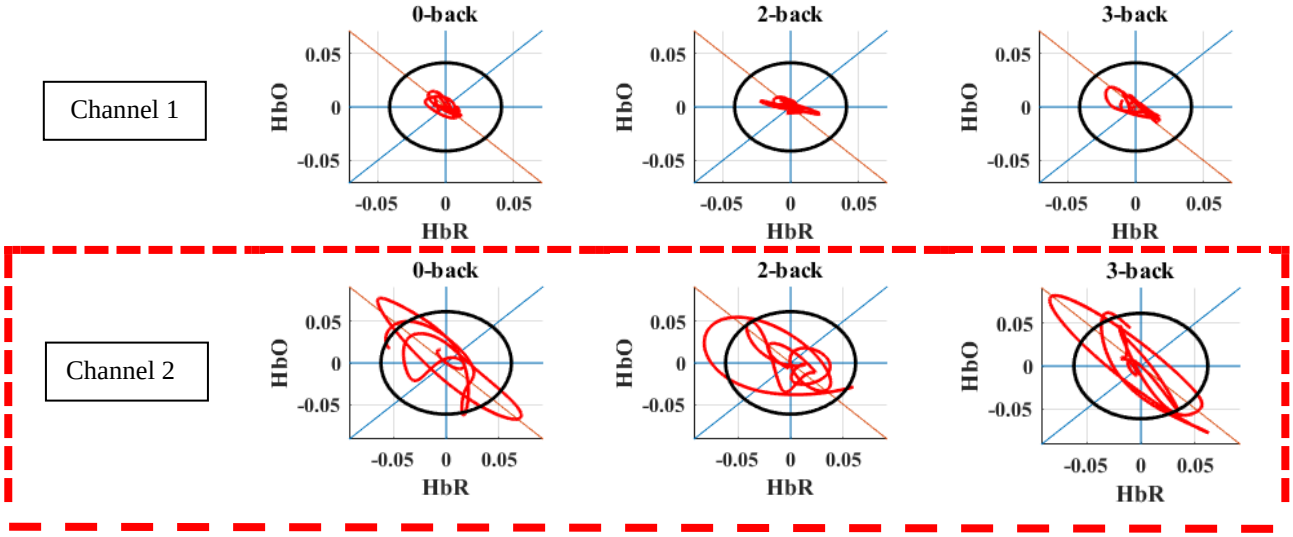

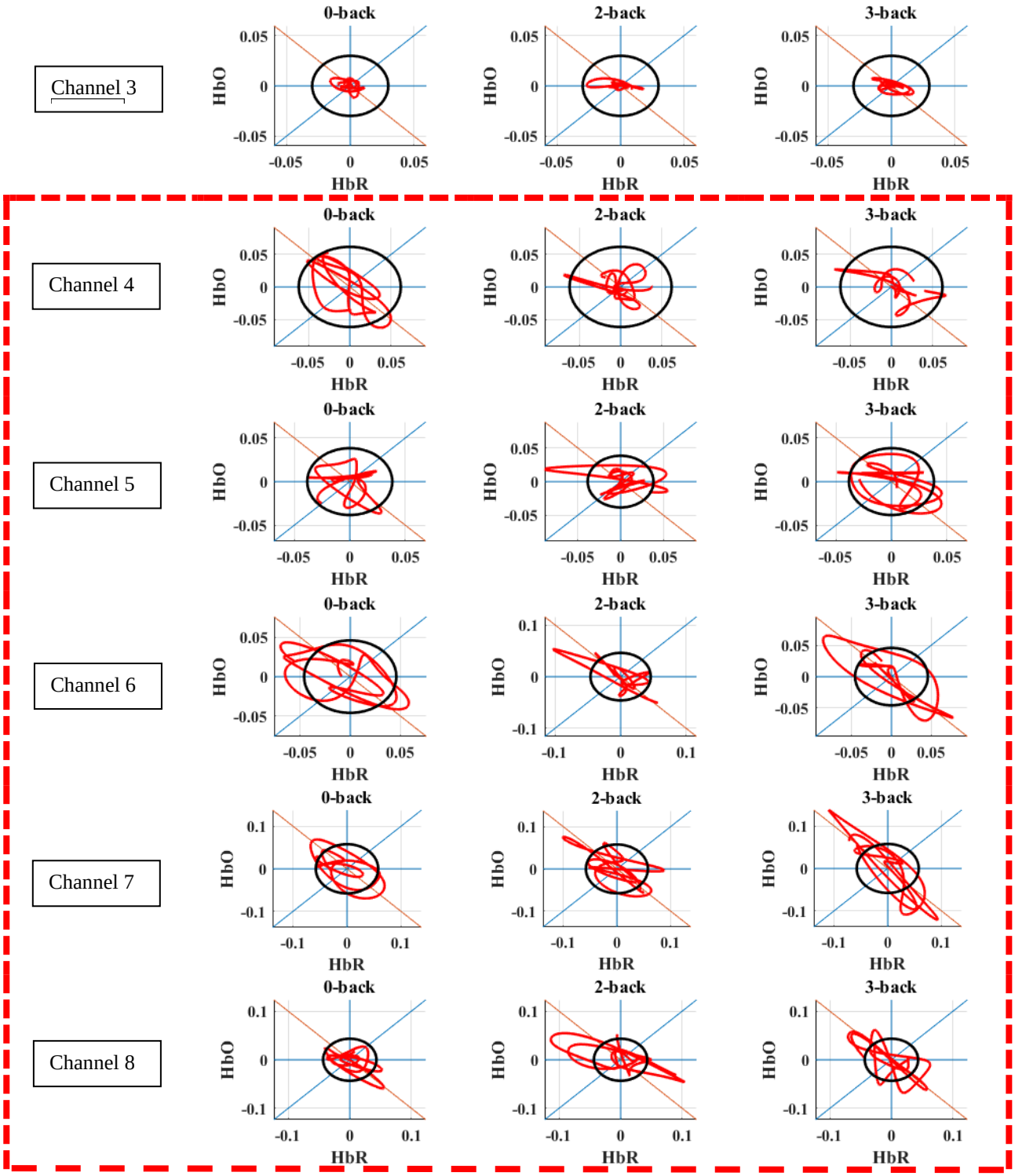
Channel 3
Channel 4
Channel 5
Channel 6
Channel 7
Channel 8
0-back
2-back
3-back
HbO
HbR

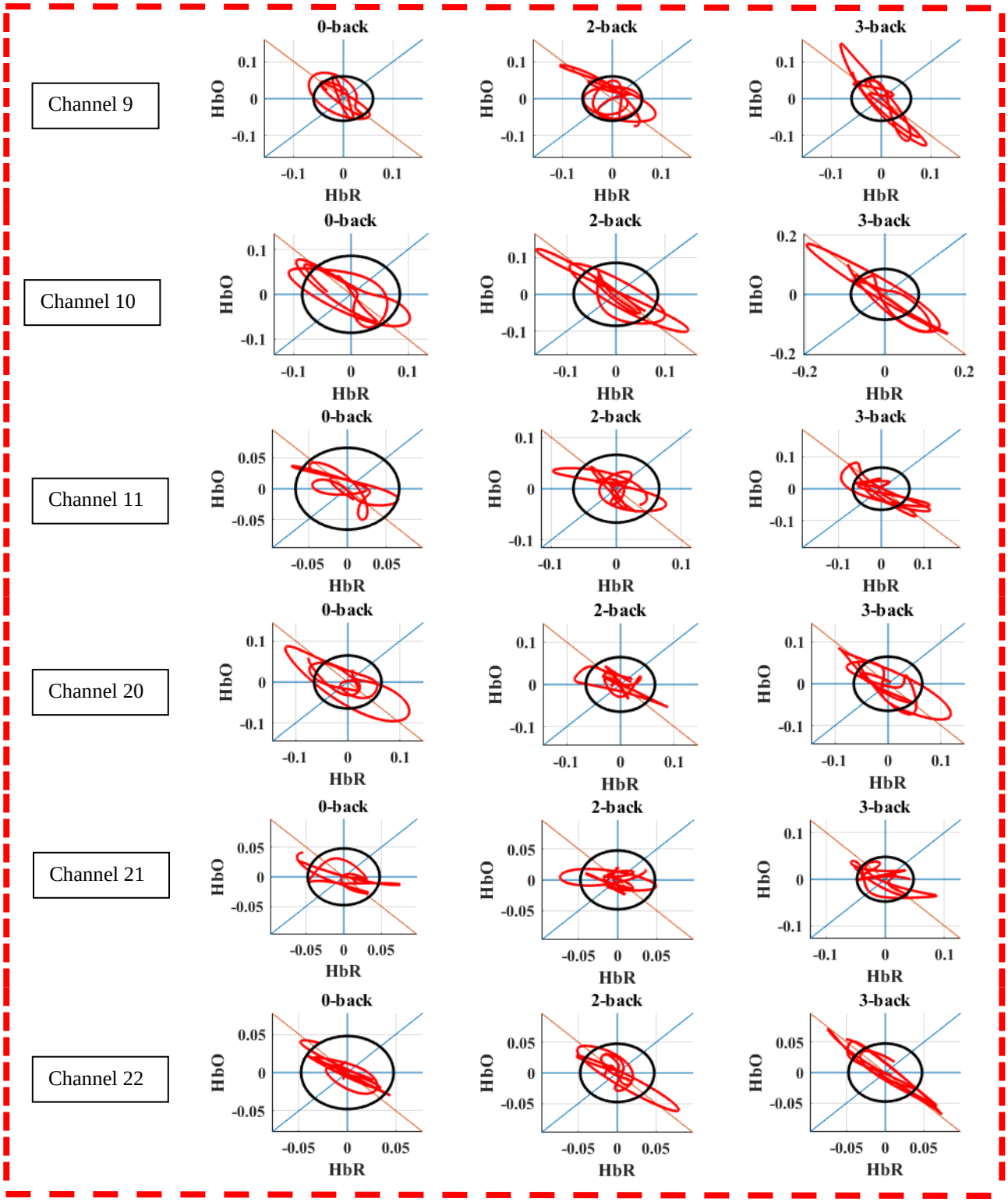
Channel 9
Channel 10
Channel 11
Channel 20
Channel 21
Channel 22
0-back
2-back
3-back
HbO
HbR

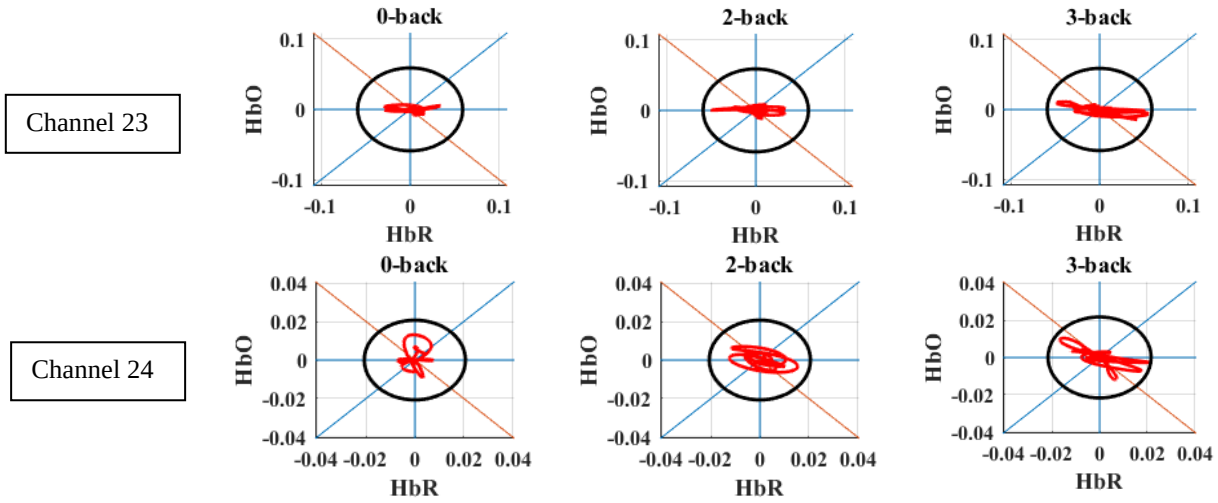

Figure 3.3: VPA Plots for fNIRS frontal channels for all 3 tasks (0-, 2- and 3-back tasks). The selected channel are the ones encaptured by dotted line boxes. (Channels 1(AF7), 2(AFF5), 3(AFp7), 4(AF5h), Channels 5(AFp3), 6(AFF3h), 7(AF1), 8(AFFz), Channels 9(AFpz), 10(AF2), 11(AFp4), 20(AFF4h), Channels 21(AF6h), 22(AFF6), 23(AFp8), 24(AF8)).

3.2.2 Data processing:

Before using the data for any technique, we have preprocessed the data to get the best possible results. For EEG data, initially all the signals were normalized using min-max normalization. Since the fundamental frequencies for this data were lying in the alpha(8-13Hz) and theta (4-8Hz) bands, so, with an intention to remove the noise and to remain within the interested frequency bands, a band pass filter (5^{th} order, Butterworth filter) of 0.1-15Hz was applied to this data to achieve the optimum outcomes. As the Figure 3.4 shows that the results of activity and rest simultaneous phase plots, using Hilbert transform, were distinguishable when this range has been used. Similarly, fNIRS data was also normalized in the beginning using min-max normalization. As the data was already in the form of HbO and HbR concentration changes (ΔHbO and ΔHbR), so there was no need to apply Beer-Lambert law. After that, a low pass filter (cut off frequency 0.2Hz, 6^{th} order, Butterworth filter) followed by a high pass filter (cutoff frequency 0.01Hz) was applied to the data to achieve signal within frequency range of 0.01-0.2Hz as the fundamental frequencies for this data were present in this band. The intention

behind applying these filters to fNIRS data was also to remove the instrumental and physiological noise present in the data.

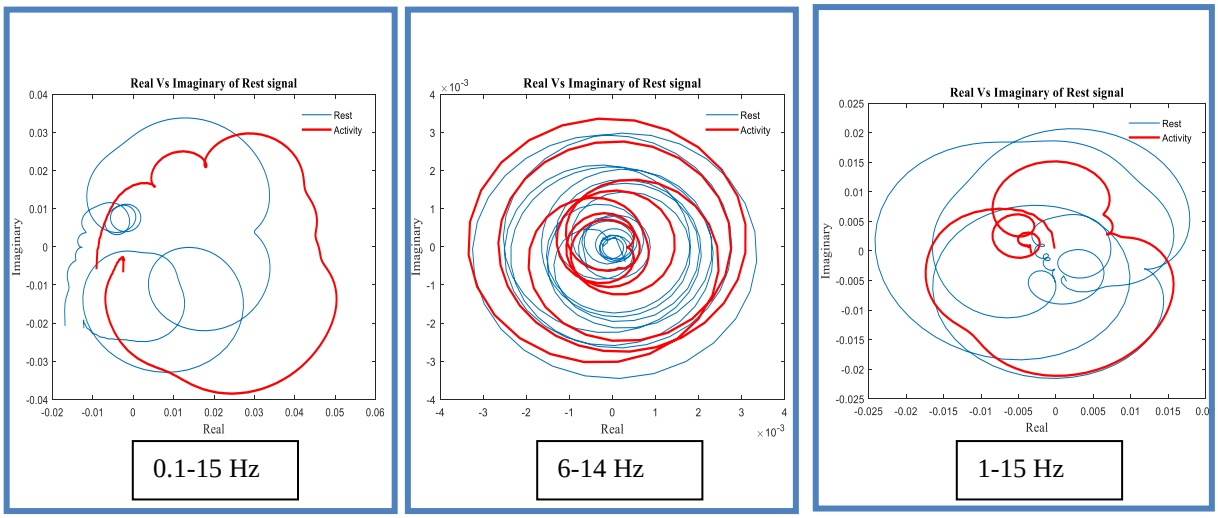

Figure 3.4: Simultaneous phase plots of rest and activity signal using Hilbert Transform

3.3 Modified multimodal (EEG-fNIRS) vector-based phase analysis:

In this study, we have proposed a modified form of vector-based phase analysis. For this study we have used just HbO and HbR to keep it simple. According to our proposed method we have drawn the threshold circle for task detection at the mean value of the resting period based on the reason that if an activity occurs than its magnitude should exceed this mean value at least. We can claim this based on the ideal HbO and HbR signals as shown in Figure 3.5. As it can be clearly observed in Figure 3.5, that when the activity starts to occur the value of HbO increases rapidly making the overall magnitude considerably greater than the mean value of baseline. We can use this mean value threshold circle for the detection of presence of activity in a series as can be seen in Figure 3.2.

So, the threshold circle's radius can be calculated as

$$\boldsymbol{r = \text{mean}\ (\sqrt{\Delta HbO^2 + \Delta HbR^2})} \qquad (12)$$

In this design, we have proposed a vector phase diagram based on both EEG and fNIRS activity detection. So, for that purpose we draw a circle for each trial activity completion in EEG signal.

As the activity can be detected earlier in EEG signal than fNIRS signal (Khan, M. J. et al., 2018), it has been deduced that if we draw a circle for the detected activity completion in each trial of EEG signal then ΔHbO and ΔHbR trajectory is expected to cross that circle if the activity is also detected in fNIRS signal. We have proposed that if fNIRS signal trajectory crosses the EEG-based circle of a trial then the activity will be considered as detected in hemodynamic response, for that trial, too. There are 20 trials in each series of EEG signal as can be observed in Figure 3.1. EEG-based circle, for each trial, is drawn in a way that when i^{th} trial activity (i =1,2,3,…20) is completed at time t_i, then values of HbO and HbR at t_i are used to calculate the magnitude $|p_i|$ of the circle. So, circle magnitude $|p_i|$ for i^{th} trial can be calculated as

$$|\boldsymbol{p_i}| = \sqrt{(\boldsymbol{HbO}|_{\boldsymbol{t_i}})^2 + (\boldsymbol{HbR}|_{\boldsymbol{t_i}})^2} \quad (13)$$

Now if the activity for any trail is detected through phase plot of EEG signal or modified VPA then it is considered as the presence of activity. The flowchart for the proposed methodology is shown in Figure 3.6. The proposed scheme can be depicted using ideal signals for both EEG and fNIRS as shown in Figure 3.7.

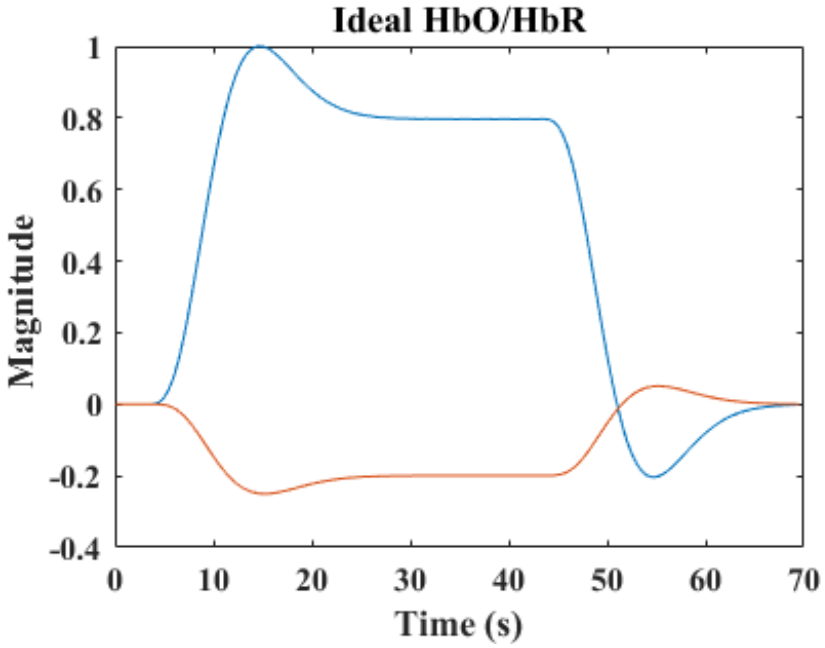

Figure 3.5: Ideal HbO/HbR signals constructed using two gamma functions

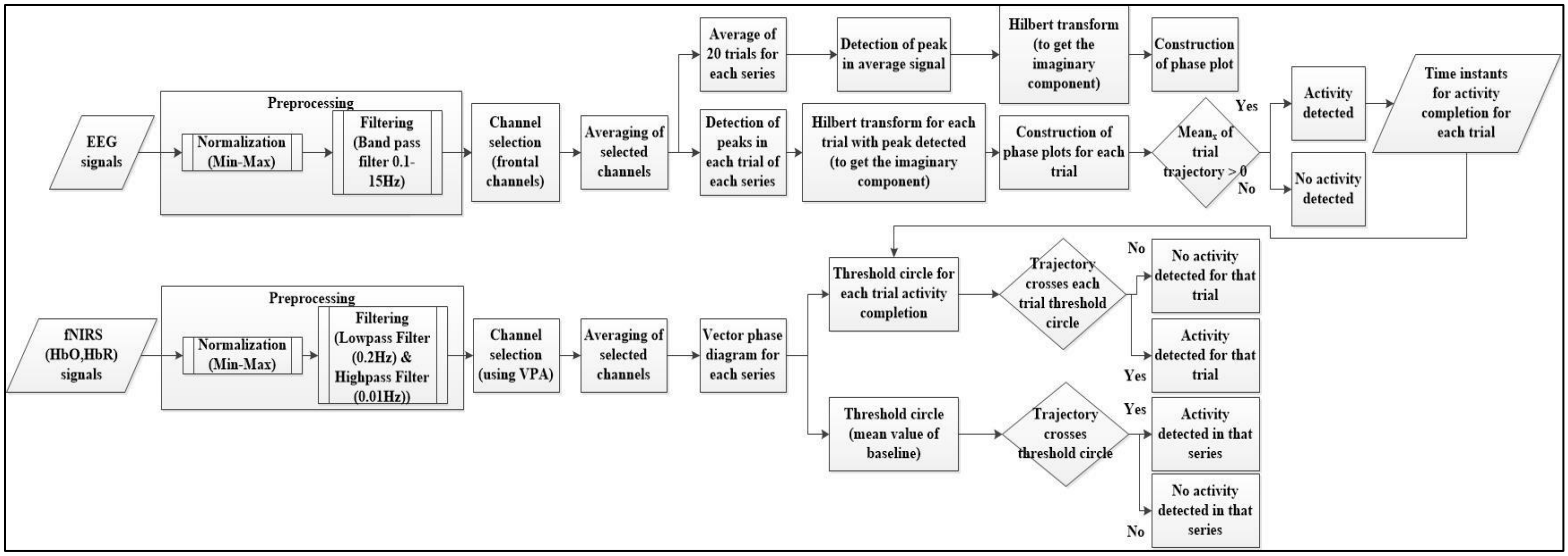

Figure 3.6: Flow diagram for the proposed scheme

3.3.1 Ideal trajectory for modified multimodal VPA:

For this experiment there were 20 trials for each series, so we convolved 20 impulses with ideal cHRF. Then it was used to construct the modified VPA as mentioned in a previous section. This approach for ideal trajectory has been depicted in Figure 3.7.

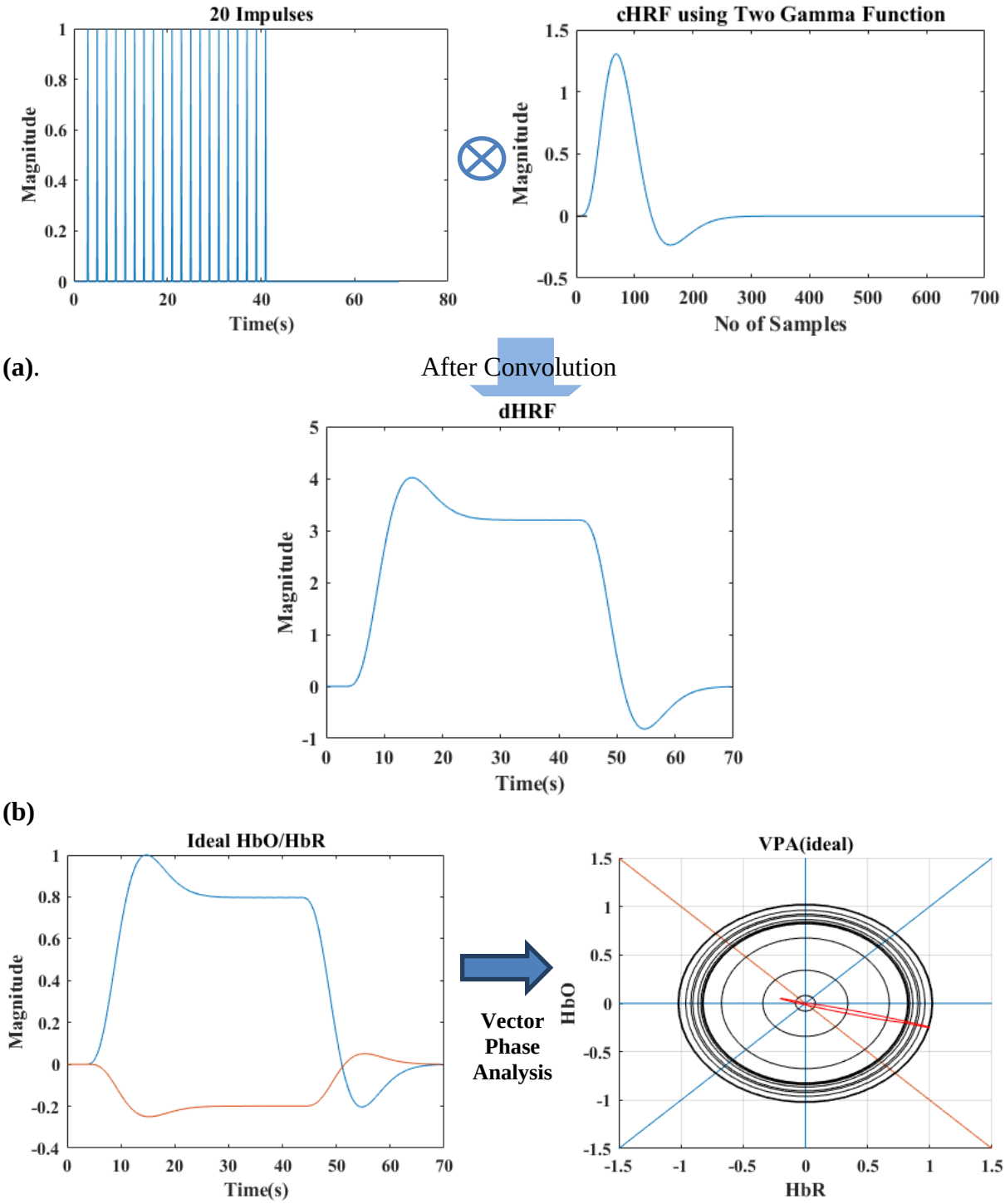

Figure 3.7: Ideal trajectory for modified VPA. (a) Ideal cHRF convolved with 20 impulses to form dHRF depicting 20 trials. (b) Ideal trajectory of HbO and HbR for modified VPA crossing all 20 circles one by one.

CHAPTER 4: RESULTS

4.1 Hilbert Transform for activity detection in EEG signals:

In this novel methodology, data from selected channels of subject 1 was initially normalized and filtered to retain data only in 0.1-15Hz frequency range as shown in Figure 4.1 and 4.2 respectively. Frequency spectrum for all the signals is shown in Figure 4.3. Then data from all channels was averaged out to construct one average signal. After that, HT is used to first calculate the imaginary component of average signal using equation (1) as shown in Figure 4.4.

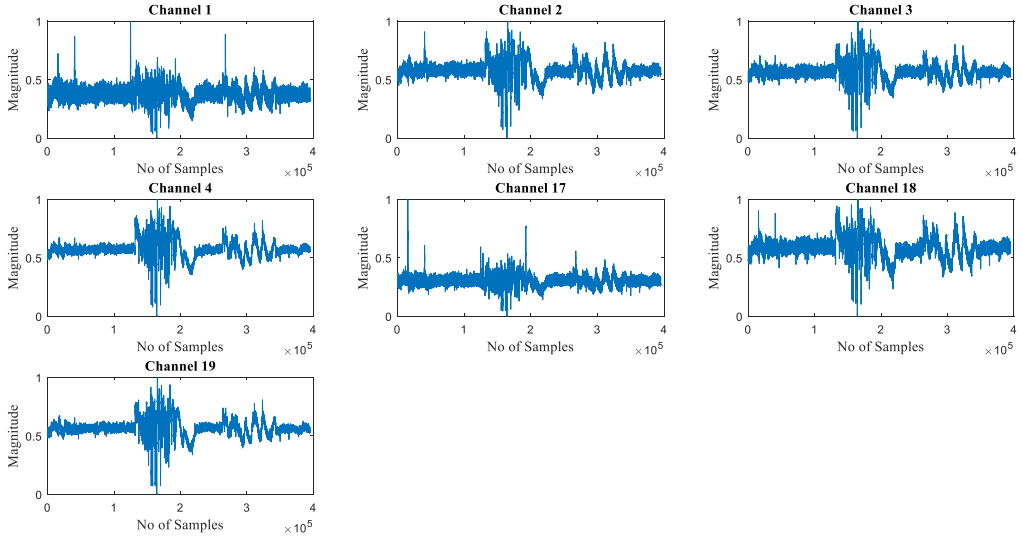

Figure 4.1: Selected EEG channels for subject 1 normalized using min-max normalization

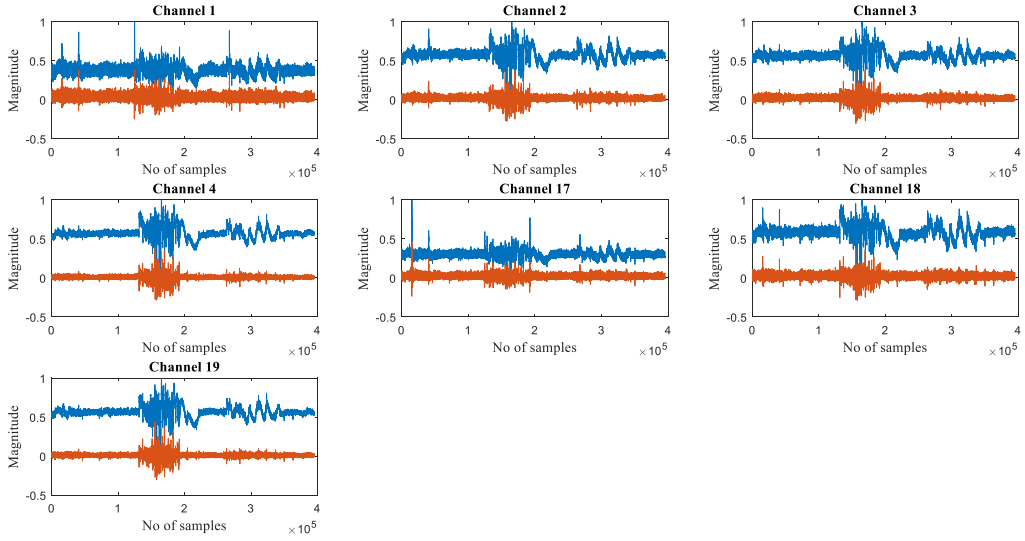

Figure 4.2: Original and filtered signals of selected EEG channels for subject 1 simultaneously plotted

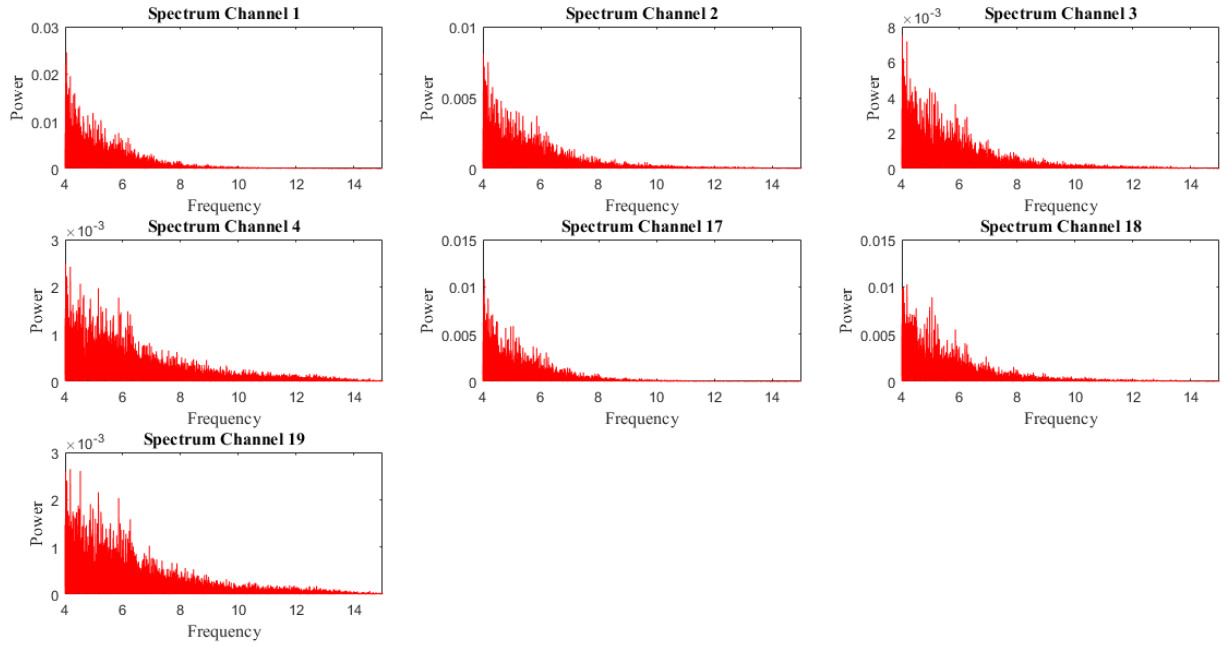

Figure 4.3: PSD of filtered EEG channels' signals

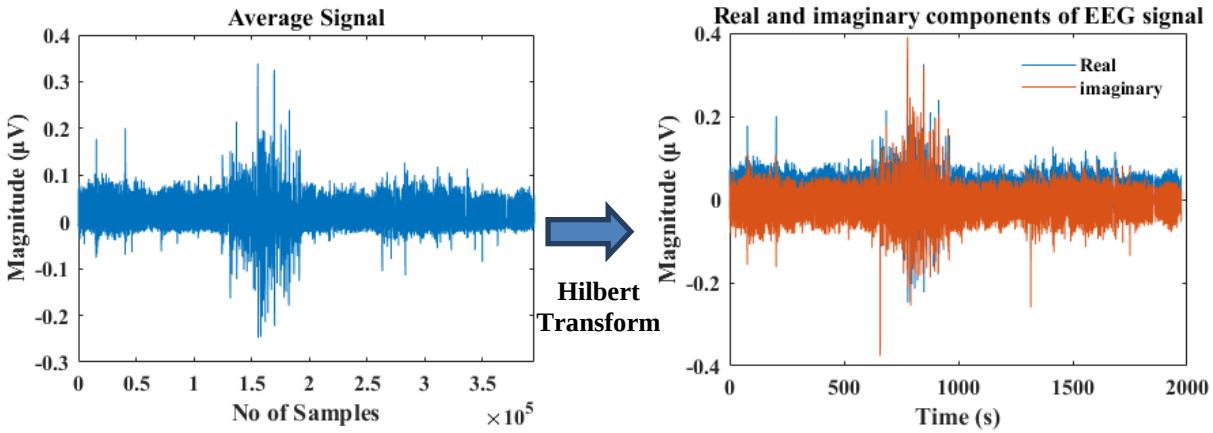

Figure 4.4: HT (Equation (1)) used to construct the imaginary component of average EEG signal.

For the 1st series of session 1, which is a 3-back task, 20 trials were averaged out and the activity portion was detected as shown in Figure 4.5. Then phase plot for the average activity signal was constructed and compared with the phase plot of rest signal. It can be clearly seen from the simultaneous phase plot of activity and rest in Figure 4.5, that the activity is contained in the right side of the plane indicating the x-coordinate of its center value as greater than 0.This proves

our claim for the criterion of activity detection in EEG signal that $mean_x$ should be greater than 0 (as mentioned in the previous section).

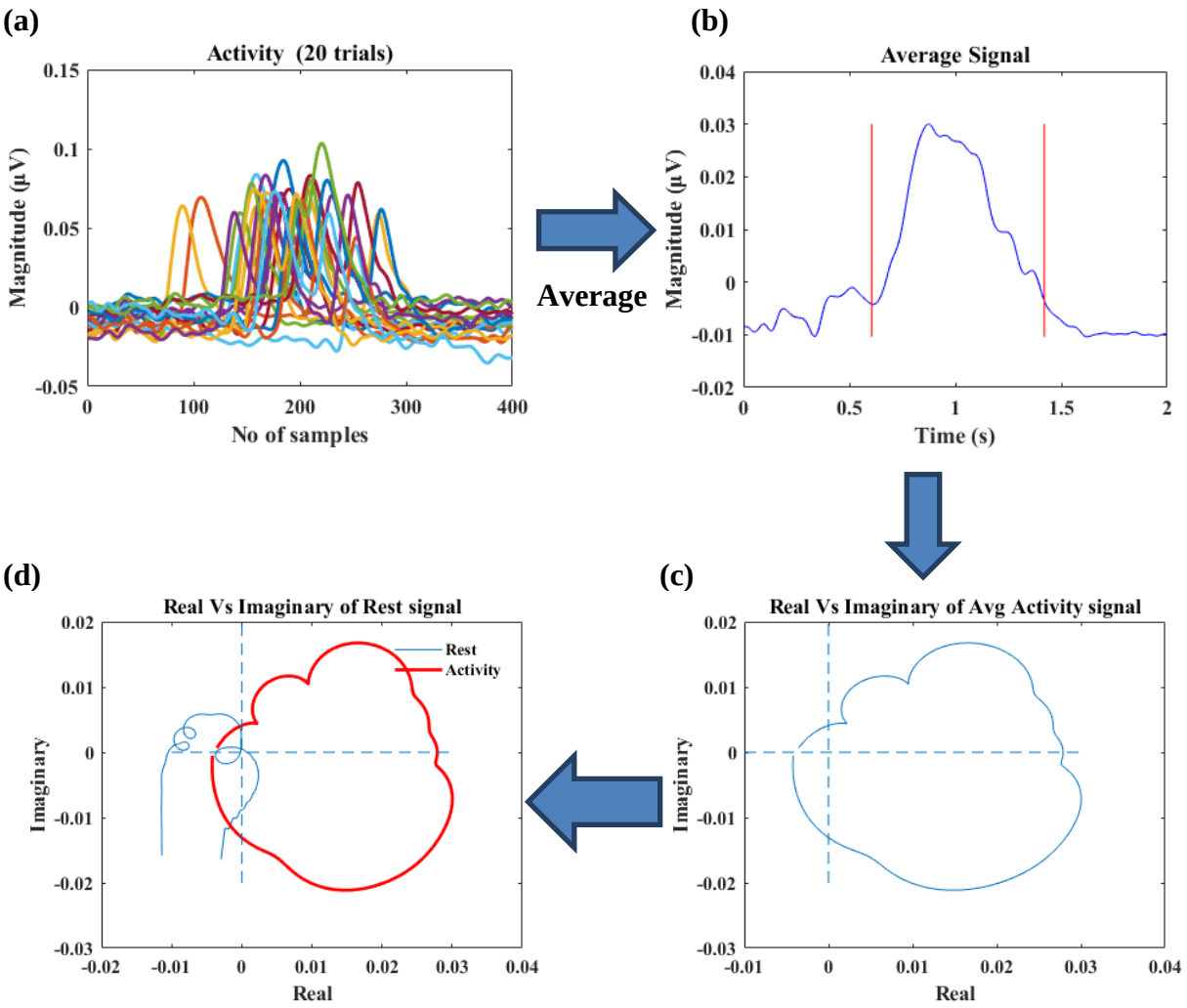

Figure 4.5: Construction of phase plots for average activity signal of 20 trials and rest signals (a) Twenty trials for series 1 of session 1 for subject 1 (b) Average activity signal of 20 trials (c) Phase plot of average activity signal (d) Simultaneous phase plot for rest and activity.

Next, we have implemented the same scheme for all the trials of series 1 as shown in Figure 4.6. Here too we can see that the trajectories for all trials are contained on the right side of the plane with $mean_x > 0$, indicating the presence of activity.

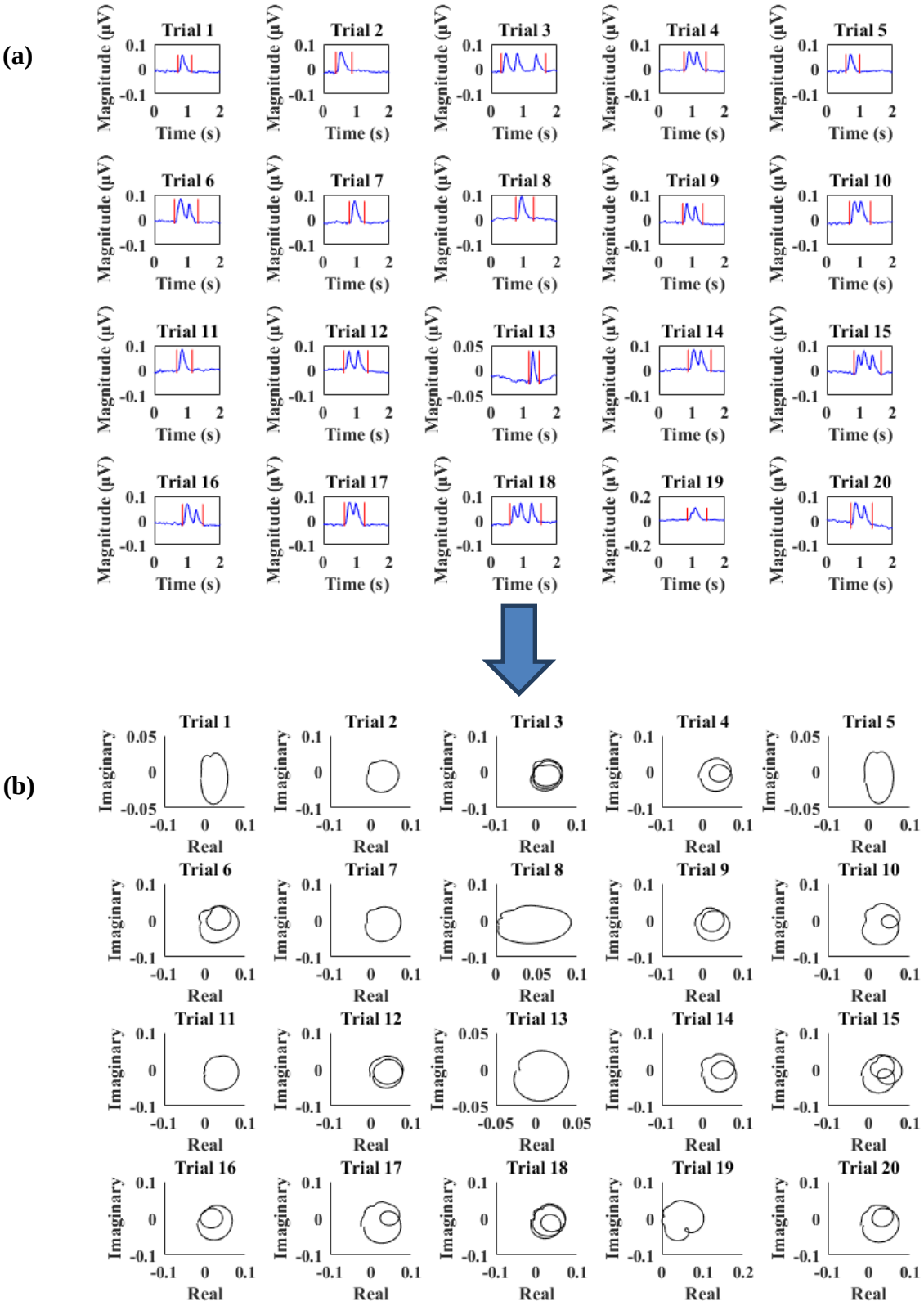

Figure 4.6: Construction of phase plots for 20 trials individually (a) Selection of activity portion in 20 trials for 1st series of 1st session for subject 1. (b) Phase plots for 20 trials using HT.

4.2 Modified VPA for hemodynamic response detection:

fNIRS signals of all selected channels, for every subject, are preprocessed and then averaged to get an average signal. Figure 4.7 displays the normalized HbO and HbR signals for selected fNIRS channels, using min-max normalization. Figure 4.8 displays the filtered HbO and HbR signals for selected channels. Figure 4.9 shows the averaged signal. Figure 4.10 shows the frequency spectrum of the average signal. As mentioned in the previous section the conventional VPA plots were constructed, for series 1 of 1st session for Subject 1, with threshold circle having radius *r*, calculated using equation (9), at the mean value of resting state as depicted in Figure 4.11(a). After that EEG-based circles were constructed for 20 trials with radii calculated using equation (10). As can be observed in Figure 4.11(b), the occurrence of activity is indicated when the HbO and HbR trajectory crosses that trial circle. When the color of trajectory turns green from red, it indicates that its magnitude is lesser than $|p_i|$, whereas when the trajectory color turns red from green it shows that its magnitude is greater than $|p_i|$, indicating the presence of activity. If the activity is either detected in EEG phase plot or in hemodynamic response, it considered as the occurrence of activity.

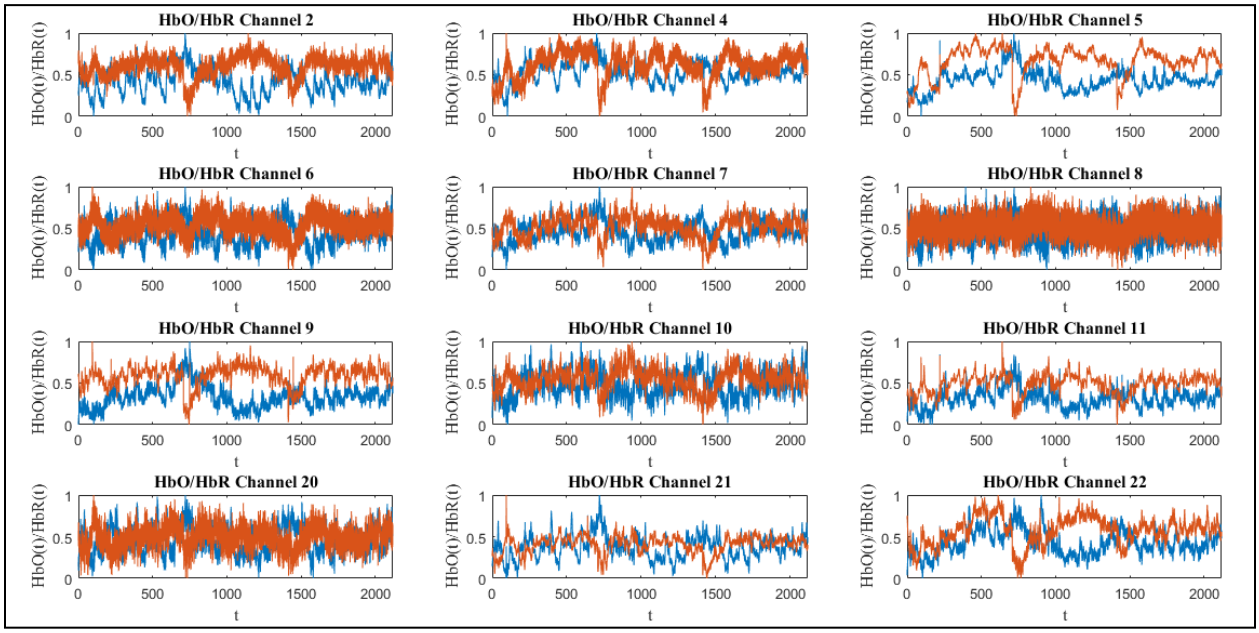

Figure 4.7: Normalized HbO and HbR signals of selected channels for subject 1

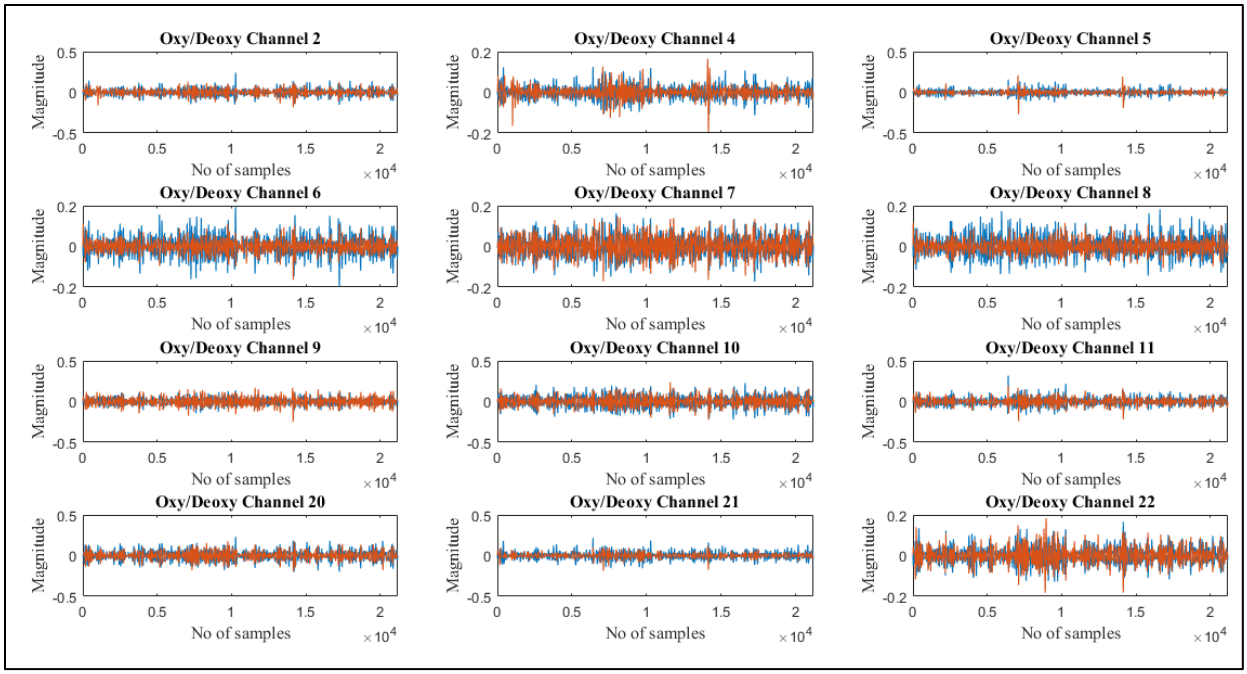

Figure 4.8: Filtered HbO and HbR signals of selected channels for subject 1

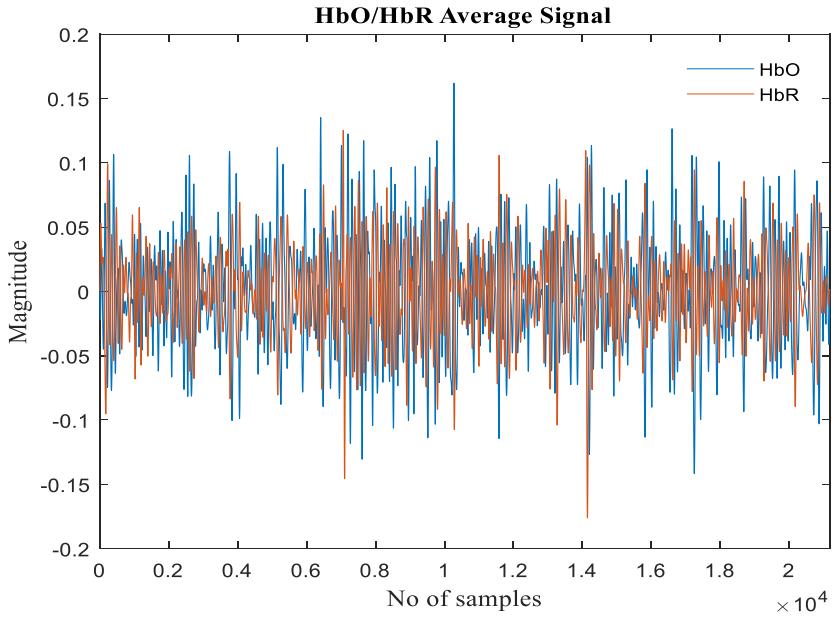

Figure 4.9: Average HbO and HbR signals, of the selected channels for subject 1, simultaneously plotted

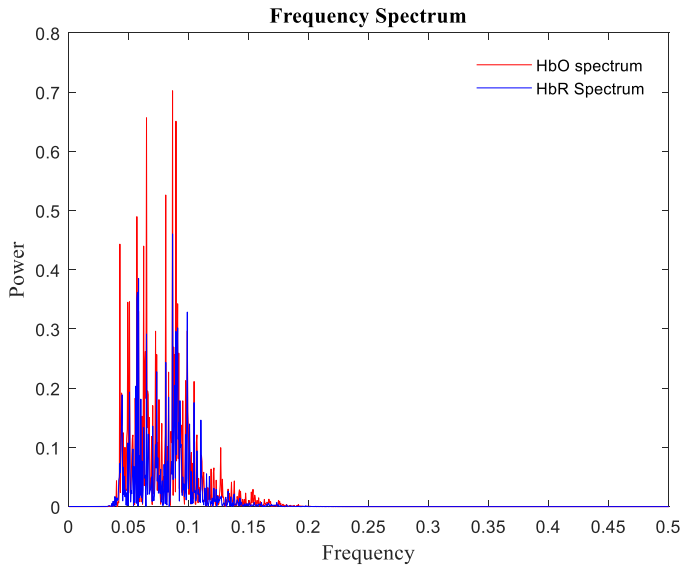

Figure 4.10: Frequency spectrum of the average signal shown in Figure 4.9

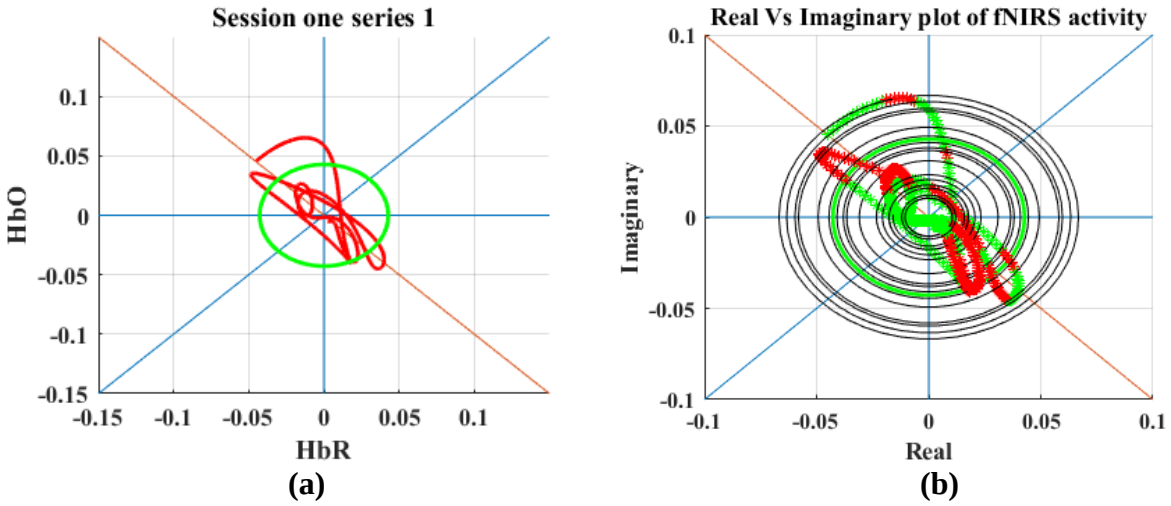

Figure 4.11: Vector phase diagrams for series 1 of session 1 for subject 1 (a) ΔHbO and ΔHbR trajectory for 1st series of 1st session for subject 1 signal with threshold circle at mean of resting state. (b) EEG-based circles for 20 trials are drawn. Trajectory color turning green from red indicates it magnitude lesser than $|p_i|$, whereas trajectory color turning red from green shows that its magnitude is greater than $|p_i|$, indicating the detection of activity in hemodynamic response.

4.3 Brain maps:

For depicting the channels' activation, we have constructed the brain maps. For this purpose, we have shown 5 brain maps of each series (0-, 2- and 3-back tasks) for 2 subjects as shown in Figure 4.12. For the construction of VPA with multiple circles for each fNIRS channel, we have chosen EEG channel closest to that particular fNIRS channel. As we are working on the frontal region of the brain, so we have selected 7 frontal EEG channels. EEG channels selected corresponding to fNIRS channels are reported in Table 4.1. We have calculated the difference of radii of 4 trials (i.e. trial no. 5,10,15,20) and rest period circles, with the radius of baseline circle individually. Using these differences, brain maps have been constructed. This method can be mathematically stated as:

$$\boldsymbol{L_{ij}} \;=\; \boldsymbol{abs}(|\boldsymbol{p_{i,j}}| - |\boldsymbol{p_{baseline,j}}|) \tag{14}$$

where L_{ij} is the difference of trial i circle radius with baseline circle radius for each channel j. For now, we have taken $i = 5, 10, 15 \;\&\; 20$ for constructing 4 maps and the 5th map is constructed based on the difference of rest period circle radius with baseline circle radius as stated below:

$$\boldsymbol{L_{rest,j}} \;=\; \boldsymbol{abs}(|\boldsymbol{p_{rest,j}}| - |\boldsymbol{p_{baseline,j}}|) \tag{15}$$

Five maps are constructed for all three types of series (0-, 2- and 3-back tasks) as shown in Figure 4.12. Presence of red color shows the highest level of activation at a brain region.

Table 4.1: EEG channels selected corresponding to fNIRS channels for the construction of brain maps

fNIRS channel No	EEG channel selected corresponding to fNIRS channel
1(AF7)	2(AFF5h)
2(AFF5)	2(AFF5h)
3(AFp7)	1(Fp1)
4(AF5h)	2(AFF5h)
5(AFp3)	1(Fp1)
6(AFF3h)	4(F1)
7(AF1)	3(AFz)
8(AFFz)	3(AFz)
9(AFpz)	3(AFz)
10(AF2)	3(AFz)
11(AFp4)	19(F2)
20(AFF4h)	17(Fp2)
21(AF6h)	18(AFF6h)
22(AFF6)	18(AFF6h)
23(AFp8)	19(F2)
24(AF8)	18(AFF6h)

(a).

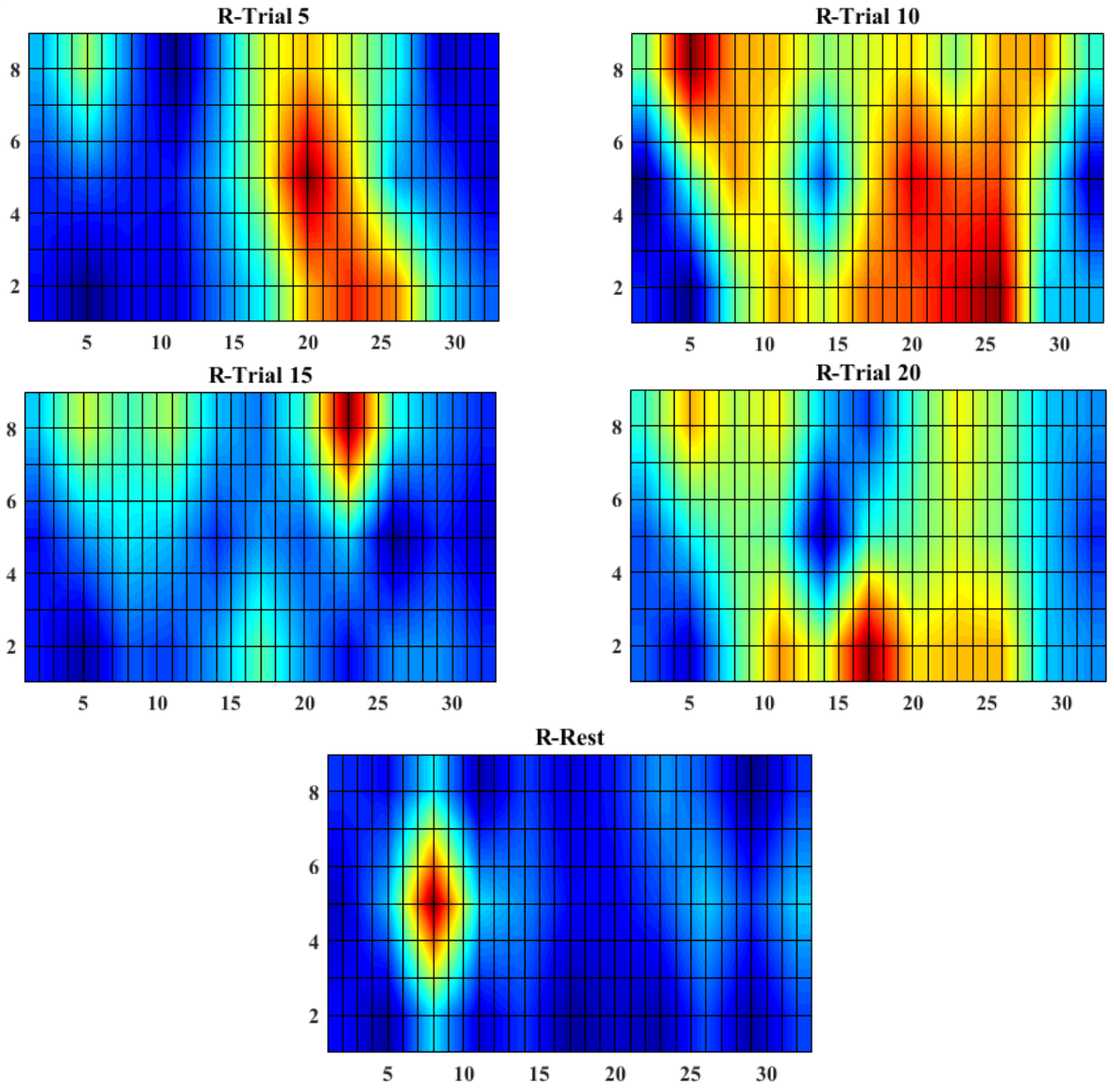
R-Trial 5
R-Trial 10
R-Trial 15
R-Trial 20
R-Rest
8
6
4
2
5
10
15
20
25
30

(b).

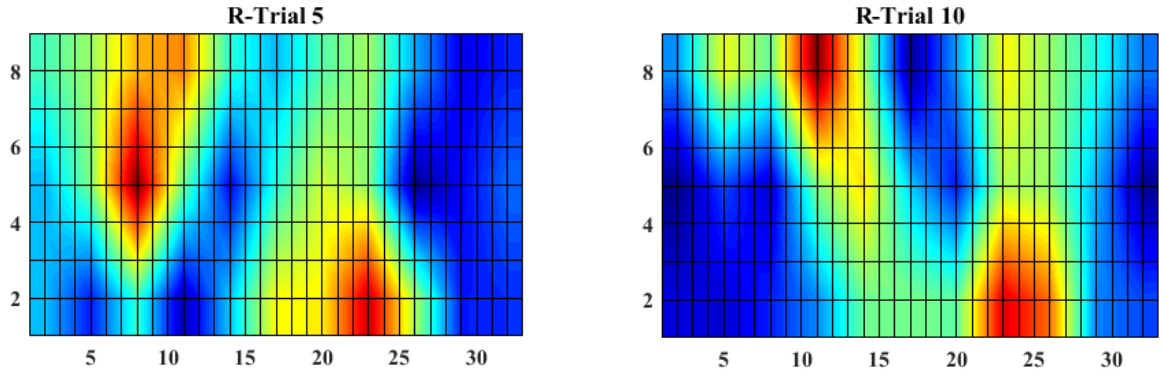
R-Trial 5
R-Trial 10
8
6
4
2
5
10
15
20
25
30

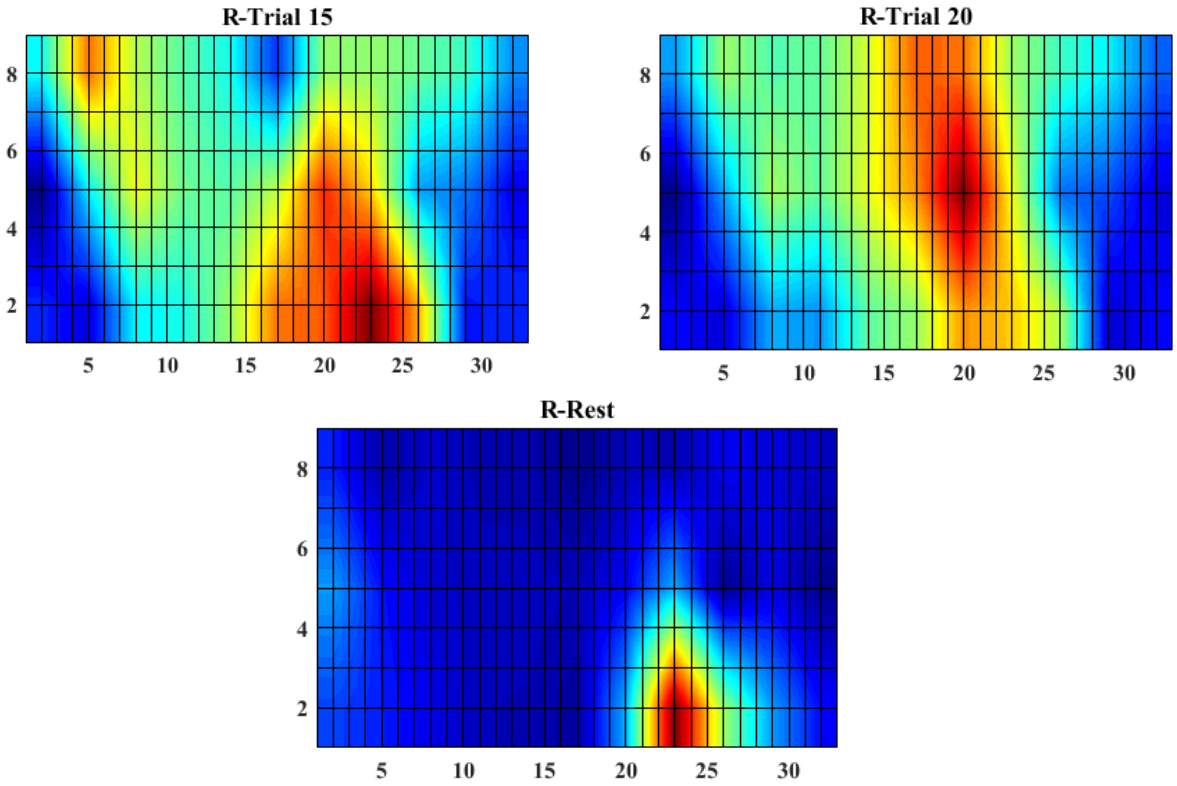
R-Trial 15
R-Trial 20
R-Rest
8
6
4
2
5
10
15
20
25
30

(c).

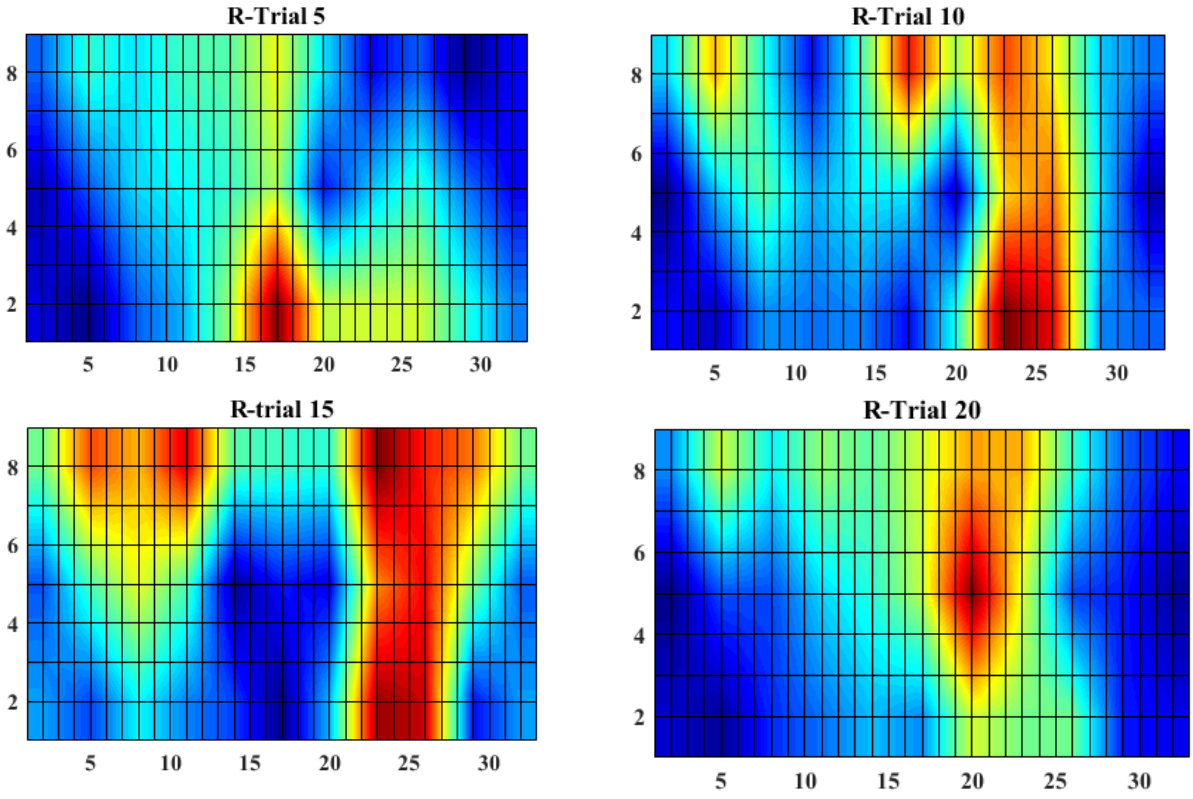
R-Trial 5
R-Trial 10
R-trial 15
R-Trial 20
8
6
4
2
5
10
15
20
25
30

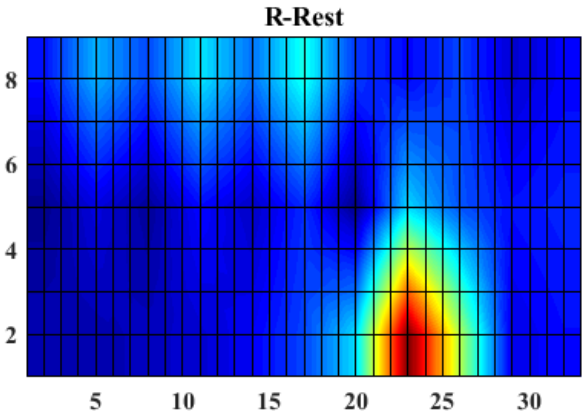
R-Rest
8
6
4
2
5
10
15
20
25
30

(d).

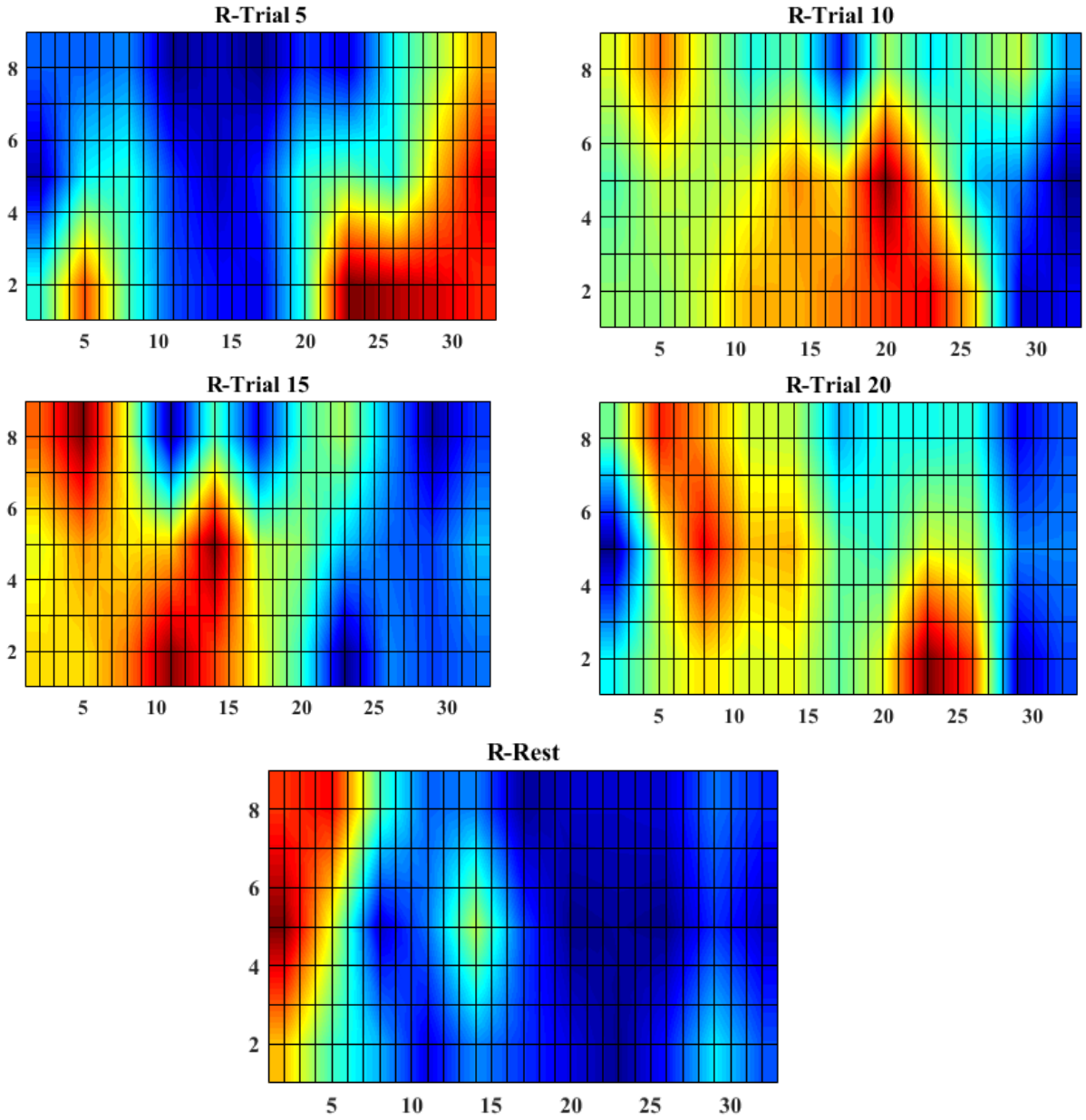
R-Trial 5
R-Trial 10
R-Trial 15
R-Trial 20
R-Rest
8
6
4
2
5
10
15
20
25
30

(e).

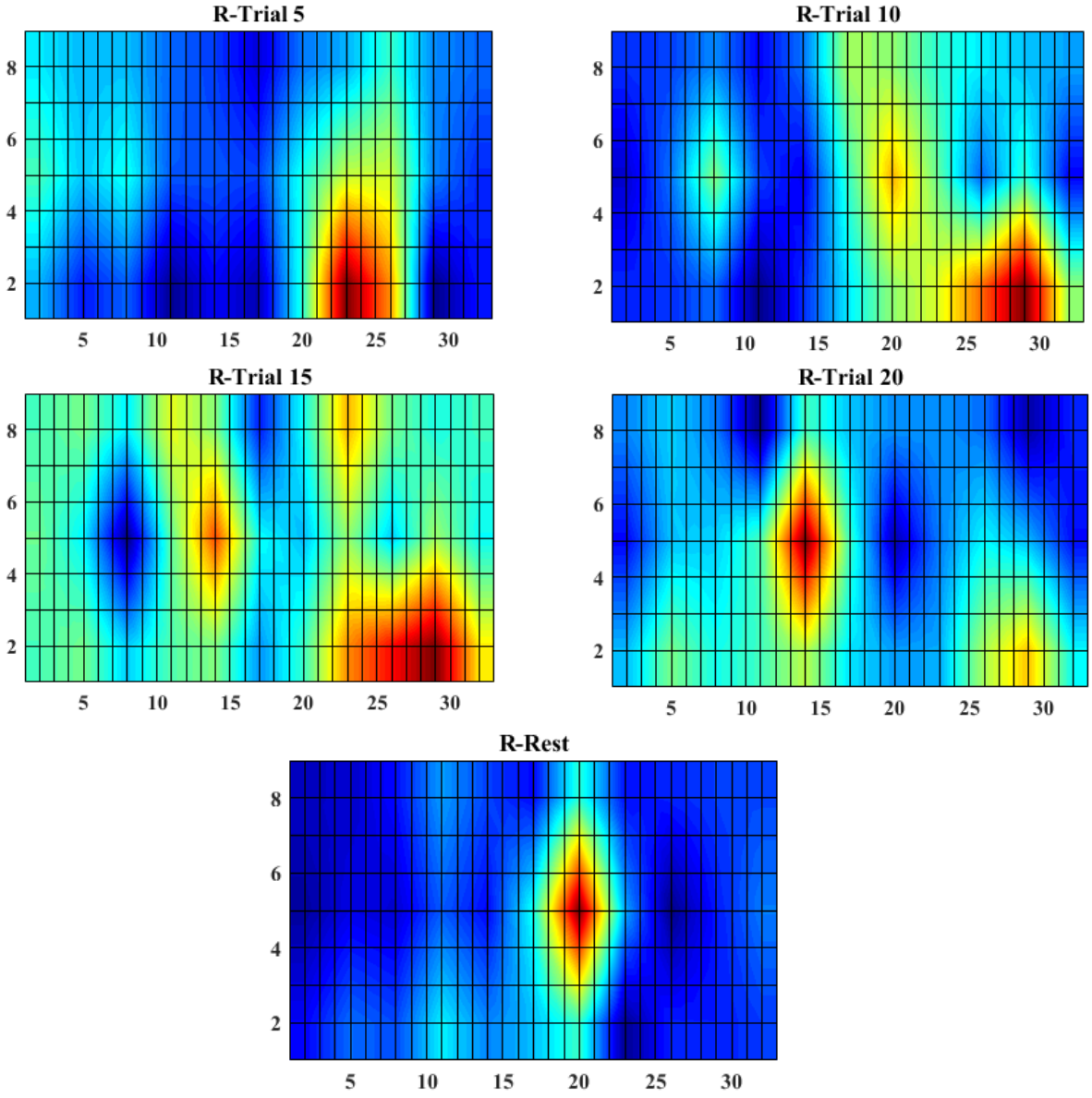
R-Trial 5
R-Trial 10
R-Trial 15
R-Trial 20
R-Rest
8
6
4
2
5
10
15
20
25
30

(f).

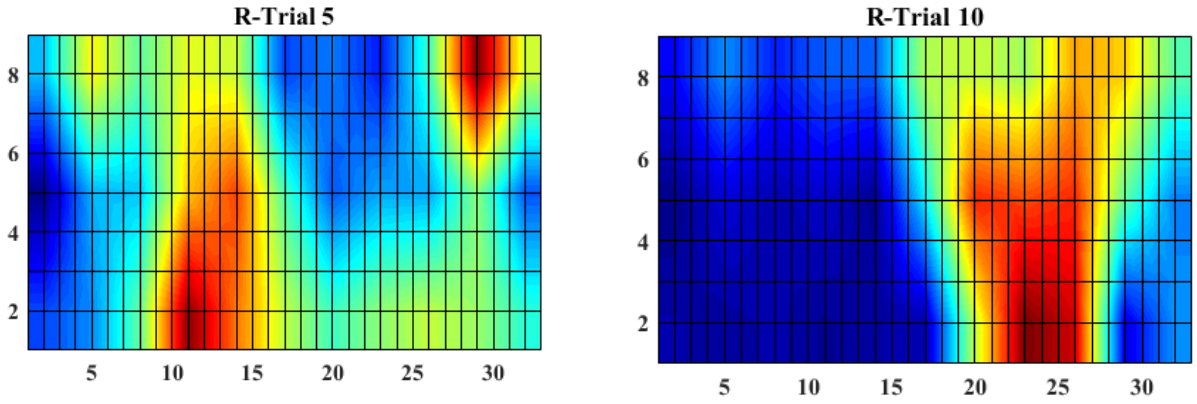
R-Trial 5
R-Trial 10
8
6
4
2
5
10
15
20
25
30

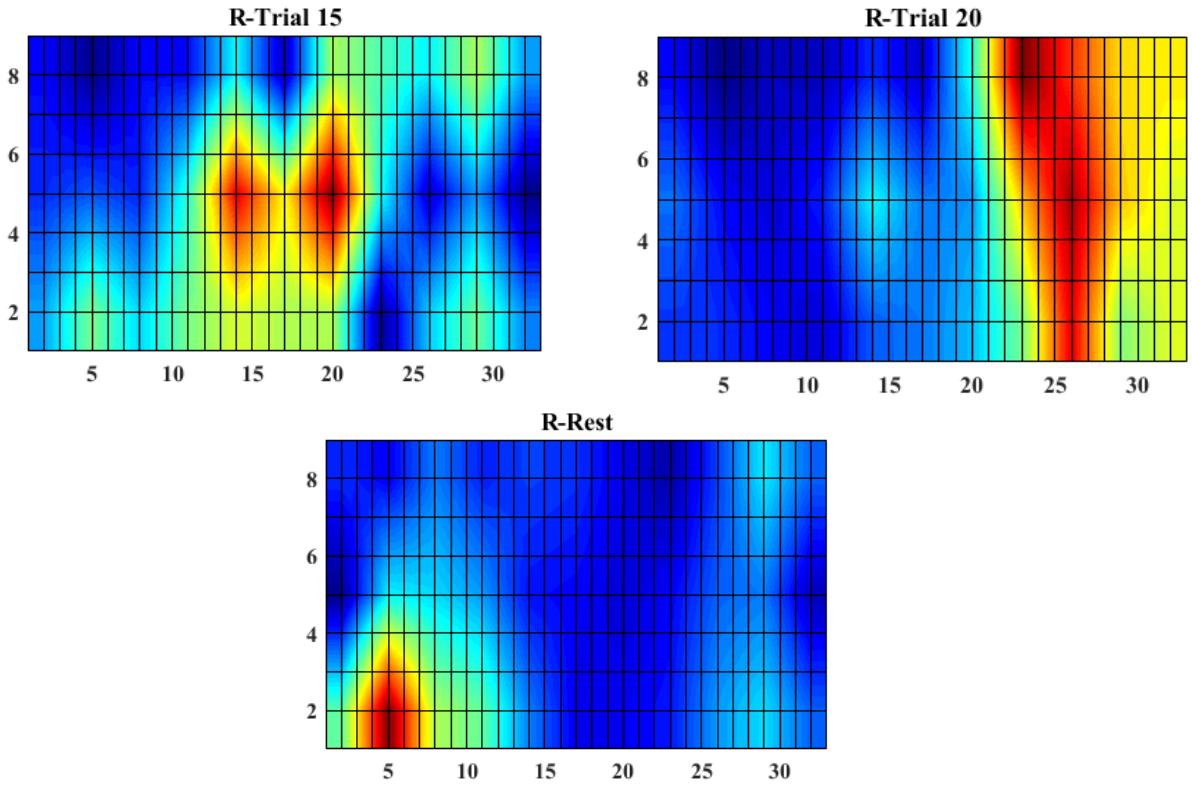

Figure 4.12: Brain Maps a) 0-back test for subject 1, b) 2-back test for subject 1, c) 3-back test for subject 1, d) 0-back test for subject 9, e) 2-back test for subject 9, f) 3-back test for subject 9.

4.4 Average classification accuracy:

After using this novel classifier for all the series of 3 sessions for all subjects, we have calculated the classification accuracies for every series. For each subject's signal all types of tasks (0-, 2- and 3- back) were performed 9 times each. So, classification accuracies for 0-back task, 2-back task and 3-back task are reported in Table 4.2, Table 4.3, and Table 4.4, respectively. The overall accuracy for this novel classifier, i.e. **91.35%** is reported in Table 4.5.

Table 4.2: Classification accuracies for 0-back task using modified multimodal VPA

Subjects	**Session 1(0-back) Accuracies (%)**			**Session 2(0-back) Accuracies (%)**			**Session 3(0-back) Accuracies (%)**			**Average Accuracy (%)**
Subject 1	100	100	100	85	75	90	95	100	90	**92.78**
Subject 2	90	90	75	90	75	90	90	85	95	**86.67**
Subject 3	80	70	75	85	85	85	90	85	95	**83.33**
Subject 4	75	65	75	80	75	75	75	55	65	**71.11**
Subject 5	100	90	90	90	95	100	80	80	90	**90.56**
Subject 6	90	85	90	85	85	70	85	90	90	**85.56**
Subject 7	90	90	75	90	90	100	90	90	75	**87.78**
Subject 8	95	95	95	95	100	95	90	95	95	**95**
Subject 9	100	100	95	95	95	100	100	100	95	**97.78**
Subject 10	80	80	75	80	75	65	80	90	80	**78.33**
Subject 11	75	85	100	90	90	95	100	95	80	**90**
Subject 12	90	65	90	100	70	85	95	90	90	**86.11**
Subject 13	95	95	95	100	95	95	95	90	90	**94.44**
Subject 14	95	95	65	80	75	95	80	80	85	**83.33**
Subject 15	95	100	95	90	95	100	90	100	85	**94.44**
Subject 16	95	95	100	95	100	95	100	100	95	**97.22**
Subject 17	100	100	100	90	95	95	95	100	100	**97.22**
Subject 18	95	85	90	80	80	90	90	80	75	**85**
Subject 19	100	100	90	100	100	100	100	100	95	**98.33**
Subject 20	95	95	95	95	85	90	85	100	80	**91.11**
Subject 21	100	95	90	100	100	100	100	100	100	**98.33**
Subject 22	85	90	85	95	80	75	85	85	95	**86.11**
Subject 23	90	100	95	95	70	95	100	90	95	**92.22**
Subject 24	85	85	90	75	95	80	85	80	80	**83.89**
Subject 25	95	100	100	100	100	100	100	100	100	**99.44**
Subject 26	80	95	100	95	80	100	90	100	85	**91.67**

Table 4.3: Classification accuracies for 2-back task using modified multimodal VPA

Subjects	**Session 1(2-back) Accuracies (%)**			**Session 2(2-back) Accuracies (%)**			**Session 3(2-back) Accuracies (%)**			**Average Accuracy (%)**
Subject 1	100	100	95	95	100	100	100	100	100	**98.89**
Subject 2	100	100	100	100	100	100	100	100	95	**99.44**
Subject 3	85	90	100	95	95	95	100	100	100	**95.56**
Subject 4	75	70	70	75	85	60	70	80	80	**73.89**
Subject 5	95	95	95	100	90	90	100	90	80	**92.78**
Subject 6	85	95	95	95	95	95	100	100	100	**95.56**
Subject 7	95	100	100	100	95	100	100	100	100	**98.89**
Subject 8	100	100	100	100	95	100	85	100	100	**97.78**
Subject 9	90	100	100	90	100	100	100	95	100	**97.22**
Subject 10	40	65	75	45	65	50	55	70	75	**60**
Subject 11	75	85	80	70	85	85	90	90	90	**83.33**
Subject 12	100	95	100	100	85	90	100	90	95	**95**
Subject 13	95	100	100	100	90	95	90	100	90	**95.56**
Subject 14	90	100	95	100	95	100	100	100	100	**97.78**
Subject 15	100	95	90	95	95	95	95	95	100	**95.56**
Subject 16	95	100	100	100	100	100	100	100	100	**99.44**
Subject 17	90	90	95	85	85	100	90	80	100	**90.56**
Subject 18	90	90	90	75	95	85	80	75	90	**85.56**
Subject 19	90	100	90	95	100	100	100	90	100	**96.11**
Subject 20	90	95	100	85	100	100	80	95	95	**93.33**
Subject 21	100	100	95	100	100	100	100	100	100	**99.44**
Subject 22	100	80	95	90	90	100	100	100	100	**95**
Subject 23	100	100	95	95	100	100	95	100	100	**98.33**
Subject 24	80	80	85	75	90	80	70	95	80	**81.67**
Subject 25	100	95	100	100	100	100	95	100	95	**98.33**
Subject 26	90	85	75	90	85	75	75	70	85	**81.11**

Table 4.4: Classification accuracies for 3-back task using modified multimodal VPA

Subjects	Session 1(3-back) Accuracies (%)			Session 2(3-back) Accuracies (%)			Session 3(3-back) Accuracies (%)			Average Accuracy (%)
Subject 1	95	100	100	85	100	95	100	100	100	**97.22**
Subject 2	95	100	100	95	100	100	100	100	100	**98.89**
Subject 3	80	100	100	100	95	95	95	100	100	**96.11**
Subject 4	85	80	80	90	75	90	80	75	70	**80.56**
Subject 5	95	100	95	95	95	100	80	85	90	**92.78**
Subject 6	70	95	85	80	85	95	95	95	100	**88.89**
Subject 7	100	100	100	100	100	100	100	100	100	**100**
Subject 8	100	100	100	100	100	95	100	100	100	**99.44**
Subject 9	100	100	100	100	100	100	95	95	95	**98.33**
Subject 10	60	65	45	65	60	60	40	55	60	**56.67**
Subject 11	90	85	75	90	95	70	90	80	90	**85**
Subject 12	100	90	85	80	85	90	75	95	90	**87.78**
Subject 13	95	95	100	95	100	100	100	85	100	**96.67**
Subject 14	100	95	100	100	100	95	100	100	100	**98.89**
Subject 15	95	100	90	100	90	100	100	100	95	**96.67**
Subject 16	95	100	100	95	100	100	95	95	100	**97.78**
Subject 17	100	90	90	95	85	100	80	100	95	**92.78**
Subject 18	75	90	80	90	80	95	80	85	80	**83.89**
Subject 19	100	95	100	100	100	100	100	100	100	**99.44**
Subject 20	85	90	95	90	90	85	95	100	100	**92.22**
Subject 21	100	100	100	100	100	95	100	100	100	**99.44**
Subject 22	90	95	95	100	95	100	95	100	95	**96.11**
Subject 23	95	95	95	100	100	100	95	100	100	**97.78**
Subject 24	80	65	80	85	70	80	85	80	75	**77.78**
Subject 25	100	100	100	95	100	95	100	100	100	**98.89**
Subject 26	75	85	65	75	80	85	95	90	80	**81.11**

Table 4.5: Average Classification accuracies for 0-, 2- and 3-back tasks using modified multimodal VPA are reported and the overall average classification accuracy of the classifier is reported to be **91.35%.**

Subjects	Average Accuracies 0-back (%)	Average Accuracies 2-back (%)	Average Accuracies 3-back (%)	Overall Average Accuracy (%)
Subject 1	92.78	98.89	97.22	**96.3**
Subject 2	86.67	99.44	98.89	**95**
Subject 3	83.33	95.56	96.11	**91.67**
Subject 4	71.11	73.89	80.56	**75.19**
Subject 5	90.56	92.78	92.78	**92.04**
Subject 6	85.56	95.56	88.89	**90**
Subject 7	87.78	98.89	100	**95.56**
Subject 8	95	97.78	99.44	**97.41**
Subject 9	97.78	97.22	98.33	**97.78**
Subject 10	78.33	60	56.67	**65**
Subject 11	90	83.33	85	**86.11**
Subject 12	86.11	95	87.78	**89.63**
Subject 13	94.44	95.56	96.67	**95.56**
Subject 14	83.33	97.78	98.89	**93.33**
Subject 15	94.44	95.56	96.67	**95.56**
Subject 16	97.22	99.44	97.78	**98.15**
Subject 17	97.22	90.56	92.78	**93.52**
Subject 18	85	85.56	83.89	**84.81**
Subject 19	98.33	96.11	99.44	**97.96**
Subject 20	91.11	93.33	92.22	**92.22**
Subject 21	98.33	99.44	99.44	**99.07**
Subject 22	86.11	95	96.11	**92.41**
Subject 23	92.22	98.33	97.78	**96.11**
Subject 24	83.89	81.67	77.78	**81.11**
Subject 25	99.44	98.33	98.89	**98.89**
Subject 26	91.67	81.11	81.11	**84.63**
Complete Average Classification Accuracy				**91.35%**

Using this novel methodology, we have achieved relatively higher average classification accuracy than other reported techniques used for this dataset and VPA with dual threshold

circles. As it can be clearly seen from Figure 4.13, that accuracy of our classifier, i.e. 91.35%, surpassed the average accuracies of VPA with dual circles (Khan, M. J. et al., 2018), SVM, CNN (Saadati et al., 2020, Asgher, Umer et al., 2020), and ERP analysis (Shin, J. et al.2018) that are 86%, 82%, 89% and 76% respectively.

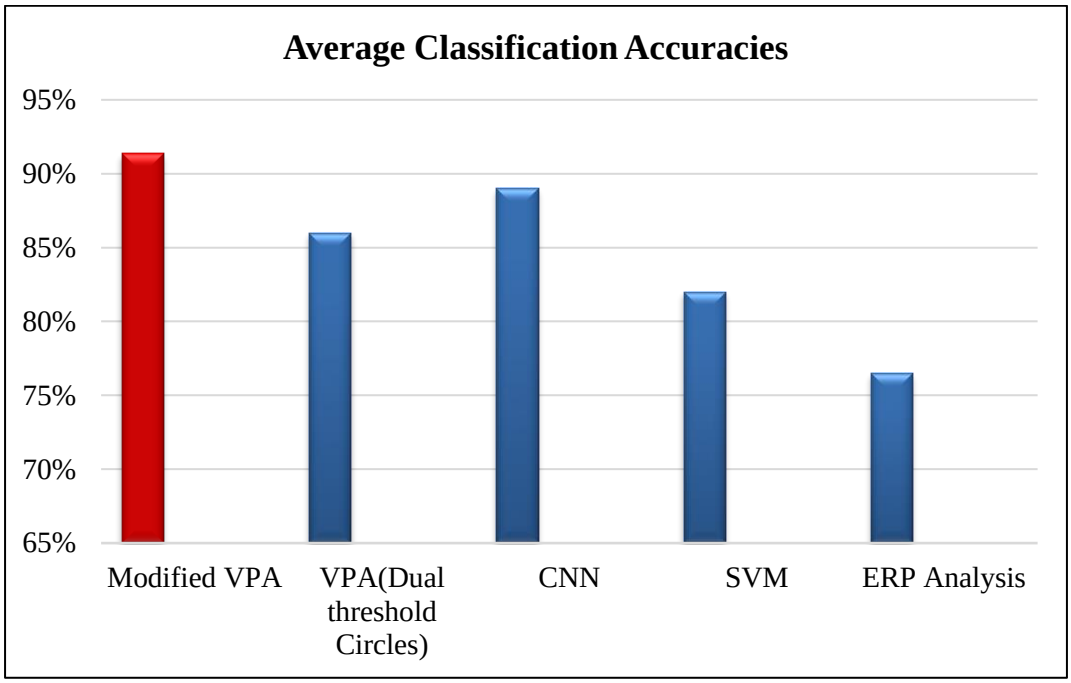

Figure 4.13: Bar chart displaying the comparison of average classification accuracies of different techniques used for multimodal data set (Shin, J et al. 2018) and VPA with dual threshold circles.

CHAPTER 5: DISCUSSION

Many researches have been carried out up till now for the purpose of improving the classification accuracy using hybrid BCI (Fazli et al., 2012, Putze, F. et al., 2014, Koo, B. et al., 2015). We have used an open-source simultaneous EEG-fNIRS dataset integrated at Technische Universität Berlin (Shin, J. et al., 2018). n-back data for fNIRS and EEG has been used to design our novel classifier. Work has been done on this dataset previously to enhance the performance accuracy. Techniques such as SVM and CNN have been implemented on n-back data and their accuracies are reported to be 82% and 89% respectively(Saadati et al., 2020, Asgher et al., 2020, Saadati et al., 2020). We have used VPA for designing our classifier, but in a modified form. An approach using VPA has already been implemented using dual threshold circles, where the first circle is the conventional resting state threshold circle, and the second circle is EEG-based circle drawn at the highest power of EEG activity window. Classification accuracy using this technique was reported to be 86% (Khan, M. J. et al., 2018). With the intention to further improve the classification accuracy of the dataset used, we have proposed a design where modified multimodal VPA with multiple EEG-based circles has been implemented. To the best of authors' knowledge, this novel classifier has been able to achieve relatively higher average classification accuracy, i.e. 91.35%, as reported in Figure 4.13.

One of the advantages of this proposed classifier is that it uses VPA for channel selection of fNIRS signals. After rejecting the inactive channels, we are averaging the selected channels' signals for each subject. Therefore, inactive channels are not contributing to reduction of signal activation, hence improving the performance making it more accurate to detect the activity in hemodynamic response.

Another advantage of this methodology is that it uses HT in a different way to construct phase plots of EEG signal trials to indicate the occurrence of activity, which is an easy and feasible method. Detection of activity in EEG separately, further enhances the performance of our classifier by increasing the average classification accuracy.

Another benefit of this classifier is that it does not require any training like other conventional machine learning and deep learning classifiers, because it is a trajectory-based approach with EEG trials- based multiple circles.

For this research, a considerably larger dataset (Shin, J et al.,2018) of 26 people have been used to design this classifier as compared to dataset of 3 people used for VPA with dual threshold circles (Khan, M. J. et al. 2018) This further strengthen the validation of the average classification accuracy achieved using our classifier.

In this study we have also highlighted the channels activation using brain maps constructed in a relatively different way than other conventional ways like t-score (Khan, M. J. et al. 2018) and z-score (Matsuda, H. et al., 2007) etc. We have constructed trial wise brain maps to show the presence of activity in different regions of brain at different stages. Our brain maps are constructed based on the difference of magnitudes of different trials' circles with the magnitude of baseline circle in vector phase diagram.

CHAPTER 6: CONCLUSION

In this study, we have proposed a novel methodology for enhancing average classification accuracy using hybrid BCI (EEG-fNIRS). For this research, we have used a hybrid (EEG-fNIRS) dataset for n-back tasks, collected at Technische Universität Berlin. Hilbert transform was used to construct phase plots for activity detection in EEG trials. A modified multimodal VPA has been designed with multiple threshold circles, drawn at the completion time of each trial activity in EEG signals, using HbO and HbR magnitudes. If the ΔHbO andΔ HbR trajectory crosses the EEG-activity-based threshold circle in the time span of each trial, then activity is considered as detected. Thus, a modified multimodal (EEG-fNIRS) VPA has been used as a classifier to get the combined accuracy for the detection of activity. The collective accuracy achieved using this novel classifier was 91.35%, relatively higher than other conventional classifiers i.e. SVM and CNN. This research is a step forward in improving the classification accuracy of state-of-the-art hybrid EEG-fNIRS BCI systems.

CHAPTER 7: FUTURE WORK

A limitation in this research is that activity in a time span is considered as detected if its occurrence is indicated in either EEG signal or multimodal VPA trajectory. A false positive detection can result in some false detection of activity. To further improve the classifier, research can be carried out to overcome this short coming.

In our proposed methodology simple preprocessing techniques have been used such as low pass, band pass and high pass filters. Presence of artifacts is still possible in the signals and can affect the resting state circle of vector phase diagram. So, to further improve the performance of this technique advanced preprocessing techniques and artifact rejection algorithms are desirable.

Moreover, in this research a comparison between gender-based accuracy has not been conducted, so this investigation can also be carried out to indicate whether the accuracy gets affected by gender or not.

APPENDIX A

MATLAB Code of VPA for Ideal HRF signal:

```
load('cnt_nback.mat')
y1=cnt_nback.x;
[m,n]=size(y1);

load('cnt_nback_fnirs.mat')
O=cnt_nback.oxy.x;
D=cnt_nback.deoxy.x;
[m1,n1]=size(O);

%%
%Markers display EEG
close all
fs=200;
x=y1(:,1);
t=(1:m)/fs;
load('mrk_nback.mat');
ti=mrk_nback.time;
tim=ones(1,length(ti));
for i=1:length(ti)
    tim(i)=ti(i)/1000;
end
plot(t,x,'b');
xlim([0 max(t)]);
title('Markers','FontSize',12,'FontName','Times');
xlabel('Time(s)','FontSize',12,'FontName','Times');
ylabel('EEG','FontSize',12,'FontName','Times');
hold on;
for i=1:567
    k=tim(i);
    line([k k],[-1000 2000],'Color','red');
end
figure;
samples=ones(1,length(tim));
for i=1:length(tim)
    samples(i)=tim(i)*fs;
end
plot(x);
xlim([0 length(x)]);
title('Markers','FontSize',12,'FontName','Times');
xlabel('No of samples','FontSize',12,'FontName','Times');
ylabel('EEG','FontSize',12,'FontName','Times');
hold on;
for i=1:567
    k=samples(i);
    line([k k],[-1000 2000],'Color','red');
end
hold off
figure;

%Markers display fnirs
fs1=10;
```

```
x2=O(:,1);
t1=(1:m1)/fs1;
load('mrk_nback_fnirs.mat');
ti1=mrk_nback.time;
tim1=ones(1,length(ti1));
for i=1:length(ti1)
    tim1(i)=ti1(i)/1000;
end
plot(t1,x2,'b');
xlim([0 max(t1)]);
title('Markers','FontSize',12,'FontName','Times');
xlabel('time(s)','FontSize',12,'FontName','Times');
ylabel('EEG','FontSize',12,'FontName','Times');
hold on;
for i=1:27
    k=tim1(i);
    line([k k],[-0.1 0.1],'Color','red');
end
hold off;
figure;
samples1=ones(1,length(tim1));
for i=1:length(tim1)
    samples1(i)=tim1(i)*fs1;
end
plot(x2);
xlim([0 length(x2)]);
title('Markers','FontSize',12,'FontName','Times');
xlabel('no of samples','FontSize',12,'FontName','Times');
ylabel('Magniude','FontSize',12,'FontName','Times');
hold on;
for i=1:27
    k=samples1(i);
    line([k k],[-0.1 0.1],'Color','red');
end
hold off;

%%
%impulse
imp=zeros(1,69.5*fs1);
m2=length(imp);
imp(1,3*fs1)=1;
for i=1:19
imp(1,fs1*(3+(i*2)))=1;
end
t2=(1:m2)/fs1;
plot(t2,imp);
title('20 Impulses','FontSize',12,'FontName','Times');
xlabel('Time(s)','FontSize',12,'FontName','Times');
ylabel('Magnitude','FontSize',12,'FontName','Times');


constants=[10 -3.6 6.6 15 0.8 1];
hrf=twogamma(constants,t2);
figure;

% convolution
```

```
res=conv(hrf,imp);
plot(t2,res(1,1:length(hrf)));
title('HRF convolved with impulses','FontSize',12,'FontName','Times');
xlabel('Time(s)','FontSize',12,'FontName','Times');
ylabel('Magnitude','FontSize',12,'FontName','Times');
figure
% normalizing hbo
mi=min(res);
ma=max(res);
for j=1:length(res)
res(j)=res(j)/ma;
end

plot(t2,res(1,1:length(t2)));

hold on;

%Construction of HbR
resR=(1/4)*(-res);
resR=[zeros(1,5) resR];
plot(t2,resR(1,1:length(hrf)));
title('Ideal HbO/HbR','FontSize',12,'FontName','Times');
xlabel('Time(s)','FontSize',12,'FontName','Times');
ylabel('Magnitude','FontSize',12,'FontName','Times');
figure
legend('HbO','HbR');
legend boxoff;
hold off;

%%
close all
%threshold circles
R=ones(1,20);
for i=1:20
   R(1,i)= (res(1,(2+(2*i))*fs1)^2 + resR(1,(2+(2*i))*fs1)^2)^(1/2);
end

%%
%plotting VPA
% u = VideoWriter('Ideal.avi');
% open(u);
xL=[-1.5,1.5];
yL=[-1.5,1.5];
line([0,0],yL);
line(xL,[0,0]);
hold on;
x=[-1.5,1.5];
y=x;
grid ON
plot(x, y);
hold on;
plot(x,-y);
title('VPA(ideal)','FontSize',12,'FontName','Times');
xlabel('HbR','FontSize',12,'FontName','Times');
ylabel('HbO','FontSize',12,'FontName','Times');
% frame = getframe(gcf);
```

```
% writeVideo(u,frame);
for i=1:20
    hold on;
    circle([0,0],R(i),'color','black');
%     frame = getframe(gcf);
%     writeVideo(u,frame);
end
hold on;
% plot(res,resR(1,1:length(res)));
curve1=animatedline('Color','r');

for i=1:length(res)
    addpoints(curve1,res(1,i),resR(1,i));
    drawnow;
%     frame = getframe(gcf);
%     writeVideo(u,frame);
end

% close(u)
```

APPENDIX B

MATLAB code for Hilbert Transform for EEG signals and multimodal VPA:

```
clc
clear all;
close all;
load('cnt_nback.mat')
y1=cnt_nback.x;
[m,n]=size(y1);
%%
% %Normalization
eeg=normalize(y1);
% Plotting Channels
s=[1 2 3 4 17 18 19];
for l=1:length(s)
    subplot(3,3,l);
    plot(eeg(:,s(l)));
    title(sprintf('Channel %d',s(l)),'FontSize',12,'FontName','Times');
    xlabel('No of Samples','FontSize',12,'FontName','Times');
    ylabel('Magnitude','FontSize',12,'FontName','Times');
end
%%
sig=zeros(6,m);

for v=1:length(s)
% close all;
 fs = 200;                                    % sample frequency (Hz)
% 10 second span time vector
%Frequency spectrum of unfiltered signals
% signal=eeg(:,s(v));
% [f,power]=Freq_spectrum(signal,fs);
% subplot(3,3,v);
% plot(f,power,'r')
% xlim([4 15]);
% title(sprintf('Spectrum Channel %d',s(v)),'FontSize',12,'FontName','Times')
% xlabel('Frequency','FontSize',12,'FontName','Times')
% ylabel('Power','FontSize',12,'FontName','Times')
%
% % figure;
[b,a]=butter(5,[0.1*2/fs 15*2/fs], 'bandpass');
xfilter=filtfilt(b,a,eeg(:,s(v)));
subplot(3,3,v);
plot(eeg(:,s(v)));
title(sprintf('Channel %d',s(v)),'FontSize',12,'FontName','Times');
xlabel('No of samples','FontSize',12,'FontName','Times');
ylabel('Magnitude','FontSize',12,'FontName','Times');
hold on
plot(xfilter);
% % legend('Original signal','filtered signal');
% % legend boxoff;
%
% % figure;
%Frequency spectrum of filtered signal
% signal=xfilter;
% [f,power]=Freq_spectrum(signal,fs);
```

```
% subplot(3,3,v);
% plot(f,power,'r')
% xlim([4 15]);
% title(sprintf('Spectrum Channel %d',s(v)),'FontSize',12,'FontName','Times')
% xlabel('Frequency','FontSize',12,'FontName','Times')
% ylabel('Power','FontSize',12,'FontName','Times')

sig(v,:)=xfilter;
end
%%
close all
eegsignal=mean(sig);
plot(eegsignal);
xlim([0 length(eegsignal)])
title('Average Signal','FontSize',12,'FontName','Times')
xlabel('No of Samples','FontSize',12,'FontName','Times')
ylabel('Magnitude','FontSize',12,'FontName','Times')
%%
% Frequency Spectrum of Avg EEG Signal
signal=eegsignal;
[f,power]=Freq_spectrum(signal,fs);
plot(f,power,'r')
xlim([4 15]);
title('Frequency Spectrum','FontSize',12,'FontName','Times')
xlabel('Frequency','FontSize',12,'FontName','Times')
ylabel('Power','FontSize',12,'FontName','Times')
%%
%Markers display EEG
close all
load('mrk_nback.mat');
ti=mrk_nback.time;
samples=disp_markers(eegsignal,ti,fs);
%%
%Hilbert Transform
close all;
t=(1:m)/fs;
plot(t,eegsignal);
title('Real and imaginary components of EEG
signal','FontSize',12,'FontName','Times');
xlabel('Time(s)','FontSize',12,'FontName','Times');
ylabel('EEG(t)','FontSize',12,'FontName','Times');
hold on;
z=hilbert(eegsignal);
w=imag(z);
plot(t,w);
legend('Real','imaginary');
legend boxoff;
hold off

figure;
plot(eegsignal(1,samples(4):samples(5)),w(1,samples(4):samples(5)),'LineWidth
',2);
hold on;
plot(eegsignal(1,samples(6):samples(7)),w(1,samples(6):samples(7)),'LineWidth
',2);
title('Task(for two 2s windows','FontSize',12,'FontName','Times');
```

```
xlabel('Real(eeg)','FontSize',12,'FontName','Times')
ylabel('Imaginary(eeg)','FontSize',12,'FontName','Times')
sno=[2 21;23 42;44 63; 65 84;86 105;107 126;128 147;149 168;170 189;191
210;212 231;233 252;254 273;275 294;296 315;317 336;338 357;359 378; 380
399;401 420;422 441;443 462;464 483;485 504;506 525;527 546;548 567];

%%
No=12;
close all;
plot(eegsignal);
title('filtered eeg signal','FontSize',12,'FontName','Times');
xlabel('No of samples','FontSize',12,'FontName','Times');
ylabel('Magnitude','FontSize',12,'FontName','Times');

g=zeros(20,400);
h=zeros(1,400);
figure;

for i=sno(No,1):sno(No,2)
    h=eegsignal(1,samples(i):samples(i)+399);
    g(i-1,:)=eegsignal(1,samples(i):samples(i)+399);
    plot(g(i-1,:), 'LineWidth',2);
    hold on;
end
title('Activity  (20 trials)','FontSize',12,'FontName','Times');
xlabel('No of samples','FontSize',12,'FontName','Times');
ylabel('Magnitude','FontSize',12,'FontName','Times');
hold off
figure;
avgsignal=mean(g);
plot(avgsignal);
title('Activity(Avg signal)','FontSize',12,'FontName','Times');
xlabel('No of samples','FontSize',12,'FontName','Times');
ylabel('Magnitude','FontSize',12,'FontName','Times');
figure;
time=(1:length(avgsignal))/fs;
plot(time,avgsignal);
title('Activity(Avg signal)','FontSize',12,'FontName','Times');
xlabel('time(s)','FontSize',12,'FontName','Times');
ylabel('Magnitude','FontSize',12,'FontName','Times');

%%
close all;
a11=avgsignal;
mi1=min(a11);
ma1=max(a11);
%
j1=1;

if (a11(1:5)>-1)
    diff=0;
else
    diff=-3;
end
while(a11(j1)<=diff)
    pa=j1;
```

```
    j1=j1+1;
    if(j1==length(a11))
        pa=length(a11);
    end
    if(j1>5)
        diff=a11(j1)-a11(j1-5);
    end
end
p1a=pa-30;
bt=p1a/fs;
% plot(a11);
% hold on
% line([p1a p1a],[mi1 ma1],'Color','red');

% figure;


[pks1,locs1]=findpeaks(a11);
findpeaks(a11);
% figure;
    for i=1:length(pks1)
        if (pks1(i)>0)
            loc1=locs1(i);
        end
    end
lo=loc1;

j=1;

if (a11(1:5)>-1)
    diff=0;
else
    diff=-3;
end
while(a11(j)<=diff)
    pb=j;
    j=j+1;
    if(j==length(a11))
        pb=length(a11);
    end
    if(j>5)
        diff=a11(j)-a11(j-5);
    end
end

p1b=pb;
b1b=a11(1,1:p1b);
avgb=mean(b1b);
maximumb=max(b1b);
while(a11(lo)>=maximumb)
    lo=lo+1;
end

if (lo>(length(a11)-30))
    sub=length(a11)-lo;
```

```
    h1b=lo+sub;
else
    h1b=lo+30;
end

ta11=(1:length(a11))/fs;
pt=h1b/fs;
plot(ta11,a11,'b');
hold on
line([pt pt],[mi1 ma1],'Color','red');
hold on
line([bt bt],[mi1 ma1],'Color','red');
title('Average Signal','FontSize',12,'FontName','Times');
xlabel('Time','FontSize',12,'FontName','Times');
ylabel('Magnitude','FontSize',12,'FontName','Times');
siga=avgsignal(1,p1a:h1b);

%%
% Task
close all
avghilbert=hilbert(siga);
avgimagi=imag(avghilbert);
plot(siga,avgimagi);
hold on
plot(mean(siga), mean(avgimagi), 'k*', 'MarkerSize', 20)
hold on;
line([0 0],[min(avgimagi) max(avgimagi)],'LineStyle','--');
hold on;
line([min(siga) max(siga)],[0 0],'LineStyle','--');
hold off;
title('Real Vs Imaginary of Avg Activity
signal','FontSize',12,'FontName','Times');
xlabel('Real','FontSize',12,'FontName','Times');
ylabel('Imaginary','FontSize',12,'FontName','Times');
%%
close all
mm=length(siga);
e=ones(1,mm);
u=ones(8,mm);
nn=mm-1;
figure;
for i=1:8
    e=eegsignal(1,samples((21*i)+1)-nn:samples((21*i)+1));
    u(i,:)=eegsignal(1,samples((21*i)+1)-nn:samples((21*i)+1));
    plot(u(i,:), 'LineWidth',2);
    hold on;
end
xlim([0 mm])
title('Rest 1s(8 windows)','FontSize',12,'FontName','Times');
xlabel('No of samples','FontSize',12,'FontName','Times');
ylabel('Magnitude','FontSize',12,'FontName','Times');
hold off
figure;
avgrest=mean(u);
plot(avgrest);
xlim([0 mm])
```

```
title('Rest(Avg signal)','FontSize',12,'FontName','Times');
xlabel('No of samples','FontSize',12,'FontName','Times');
ylabel('Magnitude','FontSize',12,'FontName','Times');
figure;
time=(1:length(avgrest))/fs;
plot(time,avgrest);
xlim([0 max(time)])
title('Rest(Avg signal)','FontSize',12,'FontName','Times');
xlabel('time(s)','FontSize',12,'FontName','Times');
ylabel('Magnitude','FontSize',12,'FontName','Times');
figure;
avghilb=hilbert(avgrest);
avgimag=imag(avghilb);
plot(avgrest,avgimag);
title('Real Vs Imaginary of Rest signal','FontSize',12,'FontName','Times');
xlabel('Real','FontSize',12,'FontName','Times');
ylabel('Imaginary','FontSize',12,'FontName','Times');
hold on;
plot(siga ,avgimagi,'r','LineWidth',2);
hold on;
line([0 0],[-0.01 0.01],'LineStyle','--');
hold on;
line([-0.01 0.01],[0 0],'LineStyle','--');
hold off;
legend('Rest','Activity');
legend boxoff;
%%
% %%
close all;
%Time values for Threshold Circles
btimes=zeros(1,20);
bsamples=zeros(1,20);
locd=zeros(1,20);
sa=sno(No,1)-1;
for z=sno(No,1):sno(No,2)
a1=eegsignal(1,samples(z):samples(z)+399);
[pks,locs]=findpeaks(a1);
%     subplot(4,5,z-ss);
%     findpeaks(a1);
    for i=1:length(pks)
        if (pks(i)>0.02)
            locd(z-sa)=locs(i);
        end
    end

lo=locd(z-sa);

if(lo>0)
mi=min(a1);
ma=max(a1);
%
j=1;
if (a1(1:5)>-1)
    diff=0;
else
    diff=-3;
```

```
end
while(a1(j)<=0.01)
    p=j;
    j=j+1;
    if(j>5)
        diff=a1(j)-a1(j-5);
    end
end

p1=p-15;
bsamples(z-sa)=p1;
btimes(z-sa)=p1/fs;
subplot(4,5,z-sa);
plot(a1);
hold on
line([p1 p1],[mi ma],'Color','red');
end
end

%%
%finding peaks
close all;
loc=zeros(1,20);
psamples=zeros(1,20);
h1=zeros(1,20);
times=zeros(1,20);
ss=sno(No,1)-1;
for z=sno(No,1):sno(No,2)
    a1=eegsignal(1,samples(z):samples(z)+399);
    [pks,locs]=findpeaks(a1);
%     subplot(4,5,z-ss);
%     findpeaks(a1);
    for i=1:length(pks)
        if (pks(i)>0.02)
            loc(z-ss)=locs(i);
        end
    end

lo=loc(z-ss);

if(lo>0)
mi=min(a1);
ma=max(a1);

j=1;
diff=-1;
while(a1(j)<=diff)
    p=j;
    j=j+1;
    if(j>10)
        diff=a1(j)-a1(j-10);
    end
end

p1=p;
b1=a1(1,1:p1);
```

```
avg=mean(b1);
maximum=max(b1);
while(a1(lo)>=maximum)
    lo=lo+1;
    if(lo>length(a11))
        lo=length(a11);
        break;
    end
end


if (lo>(length(a11)-30))
    sub1=length(a11)-lo;
    h1(z-ss)=lo+sub1;
else
    h1(z-ss)=lo+30;
end

psamples(z-ss)=h1(z-ss);
ta1=(1:length(a1))/fs;
% subplot(4,5,z-1);
% plot(a1,'b');
% hold on
% line([h(z-1) h(z-1)],[mi ma],'Color','red');
% title(sprintf('Trial %d',z-1),'FontSize',12,'FontName','Times');
% xlabel('No of Samples','FontSize',12,'FontName','Times');
% ylabel('Magnitude','FontSize',12,'FontName','Times');

times(z-ss)=h1(z-ss)/fs;
subplot(4,5,z-ss);
plot(ta1,a1,'b');
hold on
line([times(z-ss) times(z-ss)],[mi ma],'Color','red');
hold on
line([btimes(z-ss) btimes(z-ss)],[mi ma],'Color','red');
title(sprintf('Trial %d',z-ss),'FontSize',12,'FontName','Times');
xlabel('Time','FontSize',12,'FontName','Times');
ylabel('Magnitude','FontSize',12,'FontName','Times');

end

end
    %%
    close all;
centers=zeros(20,2);
ff=sno(No,1)-1;
for k1=1:20

tsignals=eegsignal(1,samples(k1+ff)+bsamples(k1):samples(k1+ff)+psamples(k1))
;
    diff3=psamples(k1)-bsamples(k1);
    if(diff3>50)
    htsignals=imag(hilbert(tsignals));
    subplot(4,5,k1);
%     plot(tsignals);
```

```
    title(sprintf('Trial %d',k1),'FontSize',12,'FontName','Times');
    xlabel('Real','FontSize',12,'FontName','Times');
    ylabel('Imaginary','FontSize',12,'FontName','Times');

    plot(tsignals,htsignals);

    hold on
    mx=mean(tsignals);
    my=mean(htsignals);
    centers(k1,1)=mx;
    centers(k1,2)=my;
    plot(mx,my, 'r*', 'MarkerSize', 5)
    end
end
  eegcounter=0;
  eegcount=zeros(1,20);
  for i=1:20
      if(centers(i,1)>0)
          eegcounter=eegcounter+1;
          eegcount(i)=1;
      else
          eegcount(i)=0;
      end
  end
%%
close all;
%FNIRS_VPA
load('cnt_nback_fnirs.mat')
O=cnt_nback.oxy.x;
D=cnt_nback.deoxy.x;
[m1,n1]=size(O);

%Normalization
Oxy=normalize(O);
Dxy=normalize(D);

for j=1:n1
   subplot(6,6,j);
   plot(Oxy(:,j));
   hold on;
   plot(Dxy(:,j));
   xlim([0 length(Oxy(:,j))]);
   title(sprintf('Channel %d',j),'FontSize',12,'FontName','Times');
end
%%
sig1=zeros(12,m1);
sig2=zeros(12,m1);
s1=[2 4 5 6 7 8 9 10 11 20 21 22];
for v=1:12
% close all;
fs1 = 10;            % Sampling frequency
T = 1/fs1;             % Sampling period
L = m;             % Length of signal
X=Oxy(:,s1(v));
Z=Dxy(:,s1(v));
```

```
t=(1:length(X))/fs1;
subplot(4,3,v);
% plot(t,X);
% hold on;
% plot(t,Z);
% xlim([0 max(t)])
% title(sprintf('HbO/HbR Channel %d',s1(v)),'FontSize',12,'FontName','Times')
% xlabel('Time','FontSize',12,'FontName','Times')
% ylabel('HbO(t)/HbR(t)','FontSize',12,'FontName','Times')
% legend('Oxy','Deoxy');
% legend boxoff;

% figure;                                % sample frequency (Hz)
% 10 second span time vector
% signal=X;
% [f1,power1]=Freq_spectrum(signal,fs1);
% signal1=Z;
% [f2,power2]=Freq_spectrum(signal1,fs1);
% plot(f1,power1,'r')
% hold on;
% plot(f2,power2,'b')
% xlim([0.05 0.5]);
% title(sprintf('Spectrum Channel
%d',s1(v)),'FontSize',12,'FontName','Times')
% xlabel('Frequency','FontSize',12,'FontName','Times')
% ylabel('Power','FontSize',12,'FontName','Times')
% legend('HbO spectrum','HbR Spectrum');
% legend boxoff;

fc=0.2;
[b,a]=butter(6,fc/(fs1/2));
xfilter1=filtfilt(b,a,X);
xfilter2=filtfilt(b,a,Z);
% % %high pass filter
hpFilt = designfilt('highpassfir','StopbandFrequency',0.005, ...
         'PassbandFrequency',0.01,'PassbandRipple',0.5, ...
         'StopbandAttenuation',65,'DesignMethod','kaiserwin');
% fvtool(hpFilt)
xfilter11=filtfilt(hpFilt,xfilter1);
xfilter22=filtfilt(hpFilt,xfilter2);
plot(xfilter11);
title(sprintf('Oxy/Deoxy Channel
%d',s1(v)),'FontSize',12,'FontName','Times');
xlabel('No of samples','FontSize',12,'FontName','Times');
ylabel('Magnitude','FontSize',12,'FontName','Times');
hold on
plot(xfilter22);
xlim([0 length(xfilter11)])

sig1(v,:)=xfilter11;
sig2(v,:)=xfilter22;
end
%%
close all
oxysig=mean(sig1);
dxysig=mean(sig2);
```

```
plot(oxysig);
hold on;
plot(dxysig);
xlim([0 length(oxysig)])
title('HbO/HbR Average Signal','FontSize',12,'FontName','Times');
xlabel('No of samples','FontSize',12,'FontName','Times');
ylabel('Magnitude','FontSize',12,'FontName','Times');
legend('HbO','HbR');
legend boxoff;
%%
%spectrums after filter
close all
fs1 = 10;                                   % sample frequency (Hz)
% 10 second span time vector
signal=oxysig;
[f3,power3]=Freq_spectrum(signal,fs1);
signal1=dxysig;
[f4,power4]=Freq_spectrum(signal1,fs1);
plot(f3,power3,'r')
hold on;
plot(f4,power4,'b')
xlim([0 0.5]);
title('Frequency Spectrum','FontSize',12,'FontName','Times')
xlabel('Frequency','FontSize',12,'FontName','Times')
ylabel('Power','FontSize',12,'FontName','Times')
legend('HbO spectrum','HbR Spectrum');
legend boxoff;

%%
%Markers display fnirs
close all
load('mrk_nback_fnirs.mat');
ti1=mrk_nback.time;
samples1=disp_markers(oxysig,ti1,fs1);
hold on;
plot(dxysig,'m');
%%
%Calculating Mag and Theta
p=ones(m1,1);
th=ones(m1,1);

for i=1:m1
    p(i,1)=(((oxysig(1,i))^2)+((dxysig(1,i))^2))^0.5;
    th(i,1)=atan(dxysig(1,i)/oxysig(1,i));
end

prest=p(samples1(2)-200:samples1(2),1);
R=mean(prest);
%%
%
%plotting
ggg=No;
close all
plot(oxysig(1,samples1(ggg):samples1(ggg)+44*fs1))
hold on
plot(dxysig(1,samples1(ggg):samples1(ggg)+44*fs1));
```

```
xlim([0 44*fs1]);
title('Session 1 series 1','FontSize',12,'FontName','Times')
xlabel('No of samples','FontSize',12,'FontName','Times');
ylabel('Magnitude','FontSize',12,'FontName','Times');
legend('HbO','HbR');
legend boxoff;
figure;
% for j=1:9
% subplot(3,4,j);
xL=[-1,1];
yL=[-1,1];
line([0,0],yL);
line(xL,[0,0]);
hold on;
x=[-1,1];
y=x;
grid ON
plot(x, y);
hold on;
plot(x,-y);
hold on;
%
plot(oxysig(1,samples1(j):samples1(j)+42*fs1),dxysig(1,samples1(j):samples1(j
)+42*fs1),'r')
plot(oxysig(1,samples1(ggg):samples1(ggg)+44*fs1),dxysig(1,samples1(ggg):samp
les1(ggg)+44*fs1),'r','LineWidth',2)
xlim([-0.15 0.15]);
ylim([-0.15 0.15]);
hold on;
circle([0,0],R,'color','green','LineWidth',2);
title(sprintf('Session one series %d',1),'FontSize',12,'FontName','Times')
xlabel('HbR','FontSize',12,'FontName','Times');
ylabel('HbO','FontSize',12,'FontName','Times');
% end

gime=zeros(1,20);
gime(1)=times(1);
for k=2:20
    gime(k)=gime(k-1)+times(k);
end
gamples=gime*fs1;
tamples=zeros(1,20);
p2=zeros(1,20);
R1=zeros(1,20);

for h=1:20
    hold on;
    tamples(h)=samples1(ggg)+gamples(h);
    p2(h)=int64(tamples(h));
    R1(h)=(((oxysig(1,p2(h)))^2)+((dxysig(1,p2(h)))^2))^0.5;
    circle([0,0],R1(h),'color','black');
end
hold off;

%%
close all;
```

```
xL=[-0.1,0.1];
yL=[-0.1,0.1];
line([0,0],yL);
line(xL,[0,0]);
hold on;
x=[-0.1,0.1];
y=x;
grid ON
plot(x, y);
hold on;
plot(x,-y);
hold on;
title('Real Vs Imaginary plot of fNIRS
activity','FontSize',12,'FontName','Times');
xlabel('Real','FontSize',12,'FontName','Times');
ylabel('Imaginary','FontSize',12,'FontName','Times');

circle([0,0],R,'color','green','LineWidth',2);

hold on;

x=1;
hh=1;
l=int64(samples1(ggg));
for i=l:l+(44*fs1)
    if(i>l+10 && rem(i,20)==0 && x<21)
        circle([0,0],R1(x),'color','black');
        hold on;
        x=x+1;
    if(x==21)
        x=20;
    end
    end

    if (p(i,1)>R1(x) )
          c = 'r*';
          kk(hh)=1;
          hh=hh+1;
    else
        c='g*';
        kk(hh)=0;
        hh=hh+1;
    end

    plot(oxysig(1,i),dxysig(1,i),c);
%    pause(0.08);
    hold on;

end
fnirscount=zeros(1,20);



for g=1:21
    o2=20*(g+1);
```

```
    o1=o2-20;
    if (mean(kk(o1:o2))==1)
        fnirscount(g+1)=0;
    elseif ( mean(kk(o1:o2))>0 && mean(kk(o1:o2))<1)
        for ee=1:20
            if (kk(o1+ee-1)==0 && kk(o1+ee)==1)
                fnirscount(g+1)=1;
                break;
%             else
%                fnirscount(g)=0;
            end

        end
    else
        fnirscount(g+1)=0;
    end
end

counter =0;
for i=1:20
 if(fnirscount(i)==1)
        counter=counter+1;
 end
end
%%
counter1 =0;
j=1;
for i=2:420
 if(kk(i-1)==0 && kk(i)==1)
        counter1=counter1+1;
        sd(j)=i;
        j=j+1;
 end
end
fnirscount1=zeros(1,20);
for i=1:length(sd)
   ki=sd/20;
   fi=floor(ki);
   fnirscount1(fi+1)=1;
end

counter2 =0;
for i=1:20
 if(fnirscount1(i)==1)
        counter2=counter2+1;
 end
end

%%
wa=0;
for u=1:20
if(fnirscount1(u)==1 || eegcount(u)==1)
    wa=wa+1;
end
end
eegcounter
```

```
counter2
accuracy=(wa/20)*100
```

MATLAB Functions:

Two Gamma Function

```
function [twogammafunction] = twogamma(array, time)

hrf1= array(1).*((time.^(array(3)-1) .* array(5).^array(3) .* exp(-
array(5)*time))./gamma(array(3)));

hrf2= (array(2).*((time.^(array(4)-1) .* array(6).^array(4) .* exp(-array(6)
* time))./(gamma(array(4)))));

hrf=hrf1+hrf2;
twogammafunction = hrf;
figure;plot(twogammafunction)
hold on;
time=1:350;
hb = plot(time/15.625,zeros(1,350),'k--');
title('cHRF using Two Gamma Function','FontSize', 12,'FontName','Times');
xlabel('No of Samples','FontSize', 12,'FontName','Times');
ylabel('Magnitude','FontSize', 12,'FontName','Times');

end
```

Normalization Function

```
function [ eeg ] = normalize(y1)
%UNTITLED2 Summary of this function goes here
%   Detailed explanation goes here

%Normalization
[m,n]=size(y1);
mini=ones(1,n);
maxi=ones(1,n);

for k=1:n
    mini(k)=min(y1(:,k));
    maxi(k)=max(y1(:,k));
end
eeg=ones(m,n);
for j=1:n
    for i=1:m
        eeg(i,j)=(y1(i,j)-mini(j))/(maxi(j)-mini(j));
    end
end
end
```

Function for Frequency Spectrum

```
function [f,power ] = Freq_spectrum( signal,fs )
%UNTITLED4 Summary of this function goes here
%   Detailed explanation goes here
y = fft(signal);
n = length(signal);          % number of samples
f = (0:n-1)*(fs/n);     % frequency range
```

```
power = abs(y).^2/n;
end
```

Function to display Markers

```
function [samples] = disp_markers(signal,ti,fs)
%UNTITLED6 Summary of this function goes here
%   Detailed explanation goes here
m=length(signal);
t=(1:m)/fs;
tim=ones(1,length(ti));
for i=1:length(ti)
    tim(i)=ti(i)/1000;
end
plot(t,signal,'b');
xlim([0 max(t)]);
title('Markers','FontSize',12,'FontName','Times');
xlabel('Time(s)','FontSize',12,'FontName','Times');
ylabel('Magnitude','FontSize',12,'FontName','Times');
hold on;
ma=max(signal);
mi=min(signal);
for i=1:length(ti)
    k=tim(i);
    line([k k],[mi ma],'Color','red');
end
figure;
samples=ones(1,length(tim));
for i=1:length(tim)
    samples(i)=tim(i)*fs;
end
plot(signal);
xlim([0 length(signal)]);
title('Markers','FontSize',12,'FontName','Times');
xlabel('No of samples','FontSize',12,'FontName','Times');
ylabel('Magnitude','FontSize',12,'FontName','Times');
hold on;
for i=1:length(ti)
    k=samples(i);
    line([k k],[mi ma],'Color','red');
end

end
```

APPENDIX C

MATLAB code for Brain Map Construction:

```
clc
% clear all;
close all
% x=load('BM.mat');
s=zeros(1,16);
j=1;
for i=3:3:48
s(j)=BM(i,5);
j=j+1;
end
 Map=[ 0 s(3) 0 s(5) 0 s(9) 0 s(11) 0 s(15) 0;
       s(1) 0 s(4) 0 s(7) 0 s(10) 0 s(13) 0 s(16);
       0 s(2) 0 s(6) 0 s(8) 0 s(12) 0 s(14) 0];
Map(2,2)=(s(1)+s(2)+s(3)+s(4))/4;
Map(2,4)=(s(4)+s(5)+s(6)+s(7))/4;
Map(2,6)=(s(7)+s(8)+s(9)+s(10))/4;
Map(2,8)=(s(10)+s(11)+s(12)+s(13))/4;
Map(2,10)=(s(13)+s(14)+s(15)+s(16))/4;
Map(1,1)=(s(1)+s(3)+Map(2,2))/3;
Map(3,1)=(s(1)+s(2)+Map(2,2))/3;
Map(1,11)=(s(15)+s(16)+Map(2,10))/3;
Map(3,11)=(s(16)+s(14)+Map(2,10))/3;
Map(1,3)=(s(3)+s(4)+s(5)+Map(2,2))/4;
Map(1,5)=(s(5)+s(7)+s(9)+Map(2,4))/4;
Map(1,7)=(s(9)+s(10)+s(11)+Map(2,6))/4;
Map(1,9)=(s(11)+s(13)+s(15)+Map(2,8))/3;
Map(3,3)=(s(2)+s(4)+s(6)+Map(2,2))/4;
Map(3,5)=(s(6)+s(7)+s(8)+Map(2,4))/4;
Map(3,7)=(s(8)+s(10)+s(12)+Map(2,6))/4;
Map(3,9)=(s(12)+s(13)+s(14)+Map(2,8))/4;
mini=min(min(BM));
maxi=max(max(BM));
colormap jet
caxis([mini maxi]);
Tnew = imresize(Map,3,'bilinear');
s1=pcolor(Tnew);
s1.FaceColor='interp';
colorbar;
```

REFERENCES

Al-Quraishi, M.S., Elamvazuthi, I., Daud, S.A., Parasuraman, S. and Borboni, A., 2018. EEG-based control for upper and lower limb exoskeletons and prostheses: A systematic review. *Sensors, 18*(10), p.3342.

Allison, B., Luth, T., Valbuena, D., Teymourian, A., Volosyak, I. and Graser, A., 2010. BCI demographics: How many (and what kinds of) people can use an SSVEP BCI?. IEEE transactions on neural systems and rehabilitation engineering, 18(2), pp.107-116.

Asgher, U., Khalil, K., Ayaz, Y., Ahmad, R. and Khan, M.J., 2020, January. Classification of Mental Workload (MWL) using Support Vector Machines (SVM) and Convolutional Neural Networks (CNN). In 2020 3rd International Conference on Computing, Mathematics and Engineering Technologies (iCoMET) (pp. 1-6). IEEE.

Beyrouthy, T., Al Kork, S.K., Korbane, J.A. and Abdulmonem, A., 2016, August. EEG mind controlled smart prosthetic arm. In 2016 IEEE international conference on emerging technologies and innovative business practices for the transformation of societies (EmergiTech) (pp. 404-409). IEEE.

Blinowska, K. and Durka, P., 2006. Electroencephalography (eeg). Wiley encyclopedia of biomedical engineering.

Chaudhary, U., Birbaumer, N. and Curado, M.R., 2015. Brain-machine interface (BMI) in paralysis. Annals of physical and rehabilitation medicine, 58(1), pp.9-13.

De Clercq, W., Lemmerling, P., Van Paesschen, W. and Van Huffel, S., 2003, September. Characterization of interictal and ictal scalp EEG signals with the Hilbert transform. In Proceedings of the 25th Annual International Conference of the IEEE Engineering in Medicine and Biology Society (IEEE Cat. No. 03CH37439) (Vol. 3, pp. 2459-2462). IEEE.

Fazli, S., Mehnert, J., Steinbrink, J., Curio, G., Villringer, A., Müller, K.R. and Blankertz, B., 2012. Enhanced performance by a hybrid NIRS–EEG brain computer interface. Neuroimage, 59(1), pp.519-529.

Hong, K.S. and Naseer, N., 2016. Reduction of delay in detecting initial dips from functional near-infrared spectroscopy signals using vector-based phase analysis. International Journal of Neural Systems, 26(03), p.1650012.

Hong, K.S. and Zafar, A., 2018. Existence of initial dip for BCI: an illusion or reality. Frontiers in neurorobotics, 12, p.69

Hong, K.S., Khan, M.J. and Hong, M.J., 2018. Feature extraction and classification methods for hybrid fNIRS-EEG brain-computer interfaces. Frontiers in human neuroscience, 12, p.246.

Kato, T., 2019. Vector-based approach for the detection of initial dips using functional near-infrared spectroscopy. London: IntechOpen.

Khan, M.J., Ghafoor, U. and Hong, K.S., 2018. Early detection of hemodynamic responses using EEG: a hybrid EEG-fNIRS study. Frontiers in human neuroscience, 12, p.479.

Khan, R.A., Naseer, N., Qureshi, N.K., Noori, F.M., Nazeer, H. and Khan, M.U., 2018. fNIRS-based Neurorobotic Interface for gait rehabilitation. Journal of neuroengineering and rehabilitation, 15(1), p.7.

Koo, B., Lee, H. G., Nam, Y., Kang, H., Koh, C. S., Shin, H. C., & Choi, S., 2015. A hybrid NIRS-EEG system for self-paced brain computer interface with online motor imagery. Journal of neuroscience methods, 244, 26–32.

Matsuda, H., Mizumura, S., Nagao, T., Ota, T., Iizuka, T., Nemoto, K., Kimura, M., Tateno, A., Ishiwata, A., Kuji, I. and Arai, H., 2007. An easy Z-score imaging system for discrimination between very early Alzheimer's disease and controls using brain perfusion SPECT in a multicentre study. Nuclear medicine communications, 28(3), pp.199-205.

Nazeer, H., Naseer, N., Khan, R.A.A., Noori, F.M., Qureshi, N.K., Khan, U.S. and Khan, M.J., 2020. Enhancing classification accuracy of fNIRS-BCI using features acquired from vector-based phase analysis. Journal of Neural Engineering.

Nicolas-Alonso, L. F. and Gomez-Gil, J., 2012. Brain computer interfaces, a review, Sensors, 12(2), pp. 1211–1279.

Oka, N., Yoshino, K., Yamamoto, K., Takahashi, H., Li, S., Sugimachi, T., Nakano, K., Suda, Y. and Kato, T., 2015. Greater activity in the frontal cortex on left curves: a vector-based fNIRS study of left and right curve driving. PLoS One, 10(5), p.e0127594.

Pfurtscheller, G., Allison, B.Z., Brunner, C., Bauernfeind, G., Solis-Escalante, T., Scherer, R., Zander, T.O., Mueller-Putz, G., Neuper, C. and Birbaumer, N., 2010. The hybrid BCI Front. Neurosci, 4, p.42.

Putze, F., Hesslinger, S., Tse, C.Y., Huang, Y., Herff, C., Guan, C. and Schultz, T., 2014. Hybrid fNIRS-EEG based classification of auditory and visual perception processes. Frontiers in neuroscience, 8, p.373.

Saadati, M., Nelson, J. and Ayaz, H., 2019, July. Convolutional neural network for hybrid fNIRS-EEG mental workload classification. In International Conference on Applied Human Factors and Ergonomics (pp. 221-232). Springer, Cham.

Sano, M., Sano, S., Oka, N., Yoshino, K., & Kato, T. (2013).' Increased oxygen load in the prefrontal cortex from mouth breathing: a vector-based near-infrared spectroscopy study'. *Neuroreport*, *24*(17), 935–940. https://doi.org/10.1097/WNR.0000000000000008

Shin, J., Von Lühmann, A., Kim, D.W., Mehnert, J., Hwang, H.J. and Müller, K.R., 2018. Simultaneous acquisition of EEG and NIRS during cognitive tasks for an open access dataset. Scientific data, 5, p.180003.

Vidaurre, C. and Blankertz, B., 2010. Towards a cure for BCI illiteracy. Brain topography, 23(2), pp.194-198.

Villringer, A., Planck, J., Hock, C., Schleinkofer, L. and Dirnagl, U., 1993. Near infrared spectroscopy (NIRS): a new tool to study hemodynamic changes during activation of brain function in human adults. Neuroscience letters, 154(1-2), pp.101-104.

Yoshino, K. and Kato, T., 2012. Vector-based phase classification of initial dips during word listening using near-infrared spectroscopy. Neuroreport, 23(16), pp.947-951.

Zafar, A. and Hong, K.S., 2017. Detection and classification of three-class initial dips from prefrontal cortex. Biomedical optics express, 8(1), pp.367-383.

Zafar, A. and Hong, K.S., 2018. Neuronal activation detection using vector phase analysis with dual threshold circles: A functional near-infrared spectroscopy study. International Journal of Neural Systems, 28(10), p.1850031.